ASC Report No. 05/2012

# Quasi-optimal a priori estimates for fluxes in mixed finite element methods and applications to the Stokes-Darcy coupling

J.M. Melenk, H. Rezaijafari, B. Wohlmuth

Institute for Analysis and Scientific Computing
Vienna University of Technology — TU Wien
www.asc.tuwien.ac.at ISBN 978-3-902627-05-6

## Most recent ASC Reports

04/2012 *M. Langer, H. Woracek*
Indefinite Hamiltonian systems whose Titchmarsh-Weyl coefficients have no finite generalized poles of non-negativity type

03/2012 *M. Aurada, M. Feischl, J. Kemetmüller, M. Page, D. Praetorius*
Adaptive FEM with inhomogeneous dirichlet data: Convergence and quasi-optimality in Rd

02/2012 *P. Goldenits, G. Hrkac, D. Praetorius, D. Suess*
An Effective Integrator for the Landau-Lifshitz-Gilbert Equation

01/2012 *A. Arnold, L. Neumann, W. Hochhauser*
Stability of glued and embedded Glass Panes: Dunkerley straight Line as a conservative Estimate of superimposed buckling Coefficients

43/2011 *G. Hastermann, P. Lima, L. Morgado, E. Weinmüller*
Numerical Solution of the Density Profile Equation with p-Laplacians

42/2011 *M. Aurada, J.M. Melenk, D. Praetorius*
Mixed Conforming elements for the large-body limit in micromagnetics: a finite element approach

41/2011 *P. Amodio, T. Levitina, G. Settanni, E.B. Weinmüller*
On the Calculation of the Finite Hankel Transform Eigenfunctions

40/2011 *D.P. Hewett, S. Langdon, J.M. Melenk*
A high frequency hp boundary element method for scattering by convex polygons

39/2011 *A. Jüngel*
Semiconductor Device Problems

38/2011 *L. Neumann, A. Arnold, W. Hochhauser*
Zur Stabilität von geklebten und geklotzten Glasscheiben: Beurteilung der Dunkerley'schen Geraden zur Beulwertbestimmung

Institute for Analysis and Scientific Computing
Vienna University of Technology
Wiedner Hauptstraße 8–10
1040 Wien, Austria

**E-Mail:** admin@asc.tuwien.ac.at
**WWW:** http://www.asc.tuwien.ac.at
**FAX:** +43-1-58801-10196

ISBN 978-3-902627-05-6

# QUASI-OPTIMAL A PRIORI ESTIMATES FOR FLUXES IN MIXED FINITE ELEMENT METHODS AND APPLICATIONS TO THE STOKES–DARCY COUPLING

J.M. MELENK*, H. REZAIJAFARI†, AND B. WOHLMUTH‡

**Abstract.** We show quasi-optimal *a priori* convergence results in the $L^2$-norm on interfaces for the approximation of the normal component of the flux in mixed finite element methods. Compared to standard estimates for this problem class, an additional factor $\sqrt{h}|\log h|$ in the *a priori* bound for the flux variable is obtained by using new upper estimates in strips of width $O(h)$ near these interfaces. An important role in the analysis play anisotropic and weighted norms. Numerical results including an application to the Darcy–Stokes coupling illustrate our theoretical results.

**AMS subject classification:** 65N30
**Key words:** anisotropic norms, local FEM error analysis, mixed finite elements, saddle point problem, Stokes–Darcy coupling, weighted norms

**1. Introduction.** An important goal of many simulations in applications are accurate and reliable values for the normal flux across certain interfaces or the boundary of the domain. As an example, we mention that the treatment of complex problems in physics or engineering requires quite often the use of a variety of models in different parts of the computational domain, which in turn are coupled through the normal flux across common interfaces. On the level of numerical methods, this entails a need to understand and quantify the discretization error in the normal flux at interfaces. In the present paper, we study this question, taking the Poisson problem in mixed form as our model problem. Our setting is motivated by more complex problems in porous media applications such as the well-known Stokes–Darcy coupling problem. There, discretizations that are (locally) conservative are of particular interest, and one such class are mixed finite element methods (FEM). An attractive feature of mixed FEM is that, in contrast to the popular, well established finite volume schemes, methods of arbitrary order are available.

In numerical methods that are based on a primal-dual formulation, the normal flux at an interface can be extracted directly from the flux variable. In mixed FEM, the errors in the primal and dual variables are linked to each other, and the standard saddle point theory [7, 18] leads to *a priori* estimates for the flux variable in the $L^2$-norm on an interface which are at most of order $l - \frac{1}{2}$, where $l$ is the order of the flux error in the $L^2$-norm on the domain. However, the *best approximation* error for the normal flux in mixed finite element methods is typically better by a factor $\sqrt{h}$. It is this gap in the *a priori* analysis that the present paper removes (up to a logarithmic factor). We flag at this point that this improved estimate is fairly easily achievable if optimal order estimates in $L^\infty$ are available; however, this requires significantly more regularity than the present analysis.

In view of the technical nature of the article, we formulate in Section 2 our model problem and state the main result which yields quasi-optimal *a priori* error estimates for the normal flux. The remainder of the paper is devoted to the proofs of the *a priori*

*(melenk@tuwien.ac.at), Institut für Analysis und Scientific Computing, Technische Universität Wien, Wiedner Hauptstrasse 8-10, A–1040 Wien, Austria
†(human.rezaijafari@ma.tum.de), M2 Zentrum Mathematik, Technische Universität München, Boltzmannstraße 3, D–85748 Garching
‡(wohlmuth@ma.tum.de), M2 Zentrum Mathematik, Technische Universität München, Boltzmannstraße 3, D–85748 Garching

bound and to numerical results. In Section 3, we introduce a suitable anisotropic norm and a dual problem with right-hand sides that are supported in a strip of width $O(h)$ near the interface. Section 3 also discusses the regularity properties of the solutions of these dual problems. Section 4 quantifies the approximation properties of the Fortin operator in these anisotropic norms. In Section 5, the convergence analysis for the dual problems is given, and the proof of the main result, Theorem 2.2, is presented. Finally, in Section 6 we provide numerical results including the application to a Stokes–Darcy coupling.

**2. Problem formulation and main results.** Let $\Omega \subset \mathbb{R}^d$, $d = 2, 3$, be a convex and bounded polyhedral domain and $f \in L^2(\Omega)$. We consider the model problem

$$-\Delta u = f \quad \text{in } \Omega, \qquad u = 0 \quad \text{on } \partial\Omega,$$

in its saddle point formulation based on $H(\text{div};\Omega)$ and $L^2(\Omega)$, where

$$H(\text{div};\Omega) := \{\tau \in L^2(\Omega)^d,\ \text{div}\,\tau \in L^2(\Omega)\}.$$

The saddle point formulation is: Find $(\sigma, u) \in H(\text{div};\Omega) \times L^2(\Omega)$ such that

$$a(\sigma, \tilde{\sigma}) + b(\tilde{\sigma}, u) = 0, \quad \tilde{\sigma} \in H(\text{div};\Omega), \tag{2.1a}$$

$$b(\sigma, \tilde{u}) = -(f, \tilde{u})_0, \quad \tilde{u} \in L^2(\Omega), \tag{2.1b}$$

where the bilinear forms $a(\cdot,\cdot)$ and $b(\cdot,\cdot)$ are given, for $\tau, \tilde{\tau} \in H(\text{div};\Omega)$ and $v \in L^2(\Omega)$, by

$$a(\tau, \tilde{\tau}) := \int_\Omega \tau \cdot \tilde{\tau}\, dx, \quad b(\tau, v) := \int_\Omega \text{div}\,\tau v\, dx.$$

The saddle point formulation is well-posed, [7, Sec. IV.1.2]. We note that in contrast to the primal weak formulation, the homogeneous Dirichlet boundary conditions do not enter into the definition of the spaces.
For integer $k \in \mathbb{N}_0$, Sobolev norms on $\Omega$ are denoted by $\|\cdot\|_k$; the semi norm $k \geq 1$ is denoted by $|\cdot|_k$. For $s \notin \mathbb{N}_0$ the Aronstein–Slobodeckij characterization for norms and semi norms is applied. A second lower index, e.g., $\|\cdot\|_{s;\omega}$ or $|\cdot|_{s;\omega}$ indicates that the norm or semi norm is not considered on $\Omega$ but on $\omega$, which will typically be an element or an edge or face. We will also work with the Besov spaces $B^s_{2,q}(\Omega)$, which are defined as interpolation spaces using the "real method" (see [21, 22] for details): for positive $s \notin \mathbb{N}$ and $q \in [1, \infty]$ we set

$$B^s_{2,q}(\Omega) := (H^{\lfloor s \rfloor}(\Omega), H^{\lceil s \rceil}(\Omega))_{s-\lfloor s \rfloor, q}. \tag{2.2}$$

**2.1. Discretization.** For simplicity of notation, we restrict ourselves to a family of quasi uniform simplicial meshes $\mathcal{T}_h$ and use standard mixed finite elements. In 2D, $\mathcal{E}_h$ stands for the set of edges whereas in 3D we write $\mathcal{E}_h$ for the set of faces. We consider the uniformly inf-sup stable pairings $V_h^k \times M_h^k \subset H(\text{div};\Omega) \times L^2(\Omega)$ where $V_h^k$ is either a Raviart–Thomas (RT) or Brezzi–Douglas–Marini (BDM) finite element space. For details, we refer to [3, 4, 7, 27] and the references therein and to the original contributions [1, 5, 6, 17, 19]. More precisely, we set

$$RT_h^k := \{\tau \in H(\text{div};\Omega),\ \tau|_T \in RT_k(T), T \in \mathcal{T}_h\}, \quad RT_k(T) := (P_k(T))^d + P_k(T)\mathbf{x}$$

$$BDM_h^k := \{\tau \in H(\text{div};\Omega),\ \tau|_T \in BDM_k(T), T \in \mathcal{T}_h\}, \quad BDM_k(T) := (P_k(T))^d,$$

where $k \in \mathbb{N}_0$ in the case of Raviart–Thomas elements and $k \in \mathbb{N}$ for Brezzi–Douglas–Marini elements. The local spaces on the element $T$ are denoted by $V_k(T)$. We recall that $RT_h^k \subset BDM_h^{k+1} \subset RT_h^{k+1}$, $k \in \mathbb{N}_0$. Quite often lowest order finite element spaces are used. The popular choice $RT_h^0$ has exactly one degree of freedom per edge/face $e \in \mathcal{E}_h$, whereas $BDM_h^1$ has two degrees of freedom per face/edge.
For the approximation of $L^2(\Omega)$, we use piecewise polynomials

$$P_h^k := \{v \in L^2(\Omega),\ v|_T \in P_k(T), T \in \mathcal{T}_h\}.$$

It is well known that the pairings $(V_h^k, M_h^k) := (RT_h^k, P_h^k)$, $k \in \mathbb{N}_0$ and $(V_h^k, M_h^k) := (BDM_h^k, P_h^{k-1})$, $k \in \mathbb{N}$ are uniformly inf-sup stable, [7, Sec. IV.1.2]. As can be easily seen, mixed finite elements satisfy the inverse estimate

$$\|\tau_h \mathbf{n}\|_{0;e} \leq \frac{C}{\sqrt{h}} \|\tau_h\|_{0;T}, \quad \tau_h \in V_k(T), \quad T \in \mathcal{T}_h, e \in \mathcal{E}_h \text{ with } e \subset \partial T. \tag{2.3}$$

We note that all our constants $0 < c, C < \infty$ are generic constants and do not depend on the mesh size but possibly depend on the order $k$.
Of crucial importance for our analysis will be the so-called Fortin operator $I_h^k$ (see, e.g., [7, Sec. III.3.3]) which maps a dense subset of $H(\text{div};\Omega)$ onto $V_h^k$. Analogously to the nodal Lagrange interpolation operator for standard conforming elements, $I_h^k \tau|_T \in V_k(T)$ is uniquely defined by $\tau$ restricted to $T$. In the case of $V_h^k = RT_h^k$, we have

$$\operatorname{div} I_h^k \tau = \Pi_h^k \operatorname{div} \tau \tag{2.4a}$$

whereas for $V_h^k = BDM_h^k$, we have

$$\operatorname{div} I_h^k \tau = \Pi_h^{k-1} \operatorname{div} \tau. \tag{2.4b}$$

Here $\Pi_h^k$ stands for the elementwise defined $L^2$-projection onto $P_h^k$. For simplicity of notation, we introduce $\Pi_h^* := \Pi_h^k$ in the case that $V_h^k = RT_h^k$ and $\Pi_h^* := \Pi_h^{k-1}$ in the case that $V_h^k = BDM_h^k$. We recall that $I_h^k$ not only commutes with $\Pi_h^*$ but also with $\pi_h^k$, i.e.,

$$(I_h^k \tau \mathbf{n})|_e = \pi_h^k (\tau \mathbf{n})|_e, \tag{2.5}$$

where $\pi_h^k$ is the $L^2$-projection onto $\prod_{e\in\mathcal{E}_h} P_k(e)$. Moreover, the Fortin operator has the following local best approximation properties, [7, Prop. 3.6, Sec. III.3.3]:

$$\|\tau - I_h^k \tau\|_{j;T} \leq C h^{s+1-j} |\tau|_{s+1;T}, \quad \tau \in (H^{s+1}(T))^d,\ 0 \leq s \leq k,\ j \in \{0,1\}, \tag{2.6a}$$

$$\|(\tau - I_h^k \tau)\mathbf{n}\|_{0;e} \leq C h^{s+1} |\tau \mathbf{n}|_{s+1;e}, \quad \tau \in H^{s+1}(e), -\frac{1}{2} \leq s \leq k. \tag{2.6b}$$

It is obvious that (2.6b) directly results from (2.5). We note that (2.6) holds for both choices of $V_h^k$ whereas for estimates in the $L^2$-norm of the divergence we have to consider, due to (2.4), the two families separately.
By $(\sigma_h, u_h) \in V_h^k \times M_h^k$ we denote the finite element solution of the mixed formulation, i.e., $(\sigma_h, u_h)$ satisfies (2.1) if the test spaces are restricted to $V_h^k$ and $M_h^k$. Moreover, $(\sigma_h, u_h) \in V_h^k \times M_h^k$ is be uniquely characterized by the following Galerkin orthogonalities:

$$a(\sigma - \sigma_h, \tilde{\sigma}_h) + b(\tilde{\sigma}_h, u - u_h) = 0, \quad \tilde{\sigma}_h \in V_h^k, \tag{2.7a}$$

$$b(\sigma - \sigma_h, \tilde{u}_h) = 0, \quad \tilde{u}_h \in M_h^k. \tag{2.7b}$$

**2.2. Main result.** The regularity assumption on $\sigma$ is formulated in terms of the Besov space $B^s_{2,1}(\Omega)$, which is defined in (2.2). We recall the fact that for each $\varepsilon > 0$ and non-integer $s$ we have the embedding $H^{s+\varepsilon}(\Omega) \subset B^s_{2,1}(\Omega) \subset H^s(\Omega)$.
Let $\Gamma$ be a $(d-1)$-manifold such that $\Omega$ is decomposed by $\Gamma$ into a finite number of Lipschitz domains. We assume that the mesh $\mathcal{T}_h$ resolves $\Gamma$. Note that we do not require that the subdomains be convex. Moreover $\Gamma$ can be written as union of $\mathcal{O}(h^{1-d})$ edges/faces in $\mathcal{E}_h$, i.e., $\overline{\Gamma} := \cup_{e\in\mathcal{E}_\Gamma\subset\mathcal{E}_h}\overline{e}$. For each $e \in \mathcal{E}_\Gamma$ we associate a unit normal $\mathbf{n}$. In the case that $e \subset \partial\Omega$, $\mathbf{n}$ is given by the outer unit normal, otherwise the orientation is arbitrary but fixed. Then we associate with each $e \in \mathcal{E}_\Gamma$ an element $T_e \in \mathcal{T}_h$ such that $e \subset \partial T_e$ and the outer unit normal of $T_e$ coincides with $\mathbf{n}$. With the aid of the elements $T_e$, we define $S_h$ as

$$\overline{S}_h := \cup_{e\in\mathcal{E}_\Gamma}\overline{T}_e. \tag{2.8}$$

and note that $S_h$ is a subset of a strip of width $\mathcal{O}(h)$ around $\Gamma$.
Lemma 2.1. *Let $(\sigma, u) \in H(\mathrm{div};\Omega)\times L^2(\Omega)$ be the solution of (2.1) and let $(\sigma_h, u_h) \in V_h^k \times M_h^k$ be its finite element approximation determined by (2.7). If $\sigma \in (B_{2,1}^{k+\frac{3}{2}}(\Omega))^d$, then the $L^2$-norm error of the flux on the interface $\Gamma$ can be bounded by*

$$\|(\sigma-\sigma_h)\mathbf{n}\|_{0;\Gamma} \le C\left(h^{k+1}\|\sigma\|_{B_{2,1}^{k+\frac{3}{2}}} + \frac{1}{\sqrt{h}}\|\sigma-\sigma_h\|_{0;S_h}\right),$$

*where $\|\cdot\|_{B_{2,1}^{k+\frac{3}{2}}}$ stands for the Besov space $(B_{2,1}^{k+\frac{3}{2}}(\Omega))^d$-norm.*
*Proof.* Starting with the triangle inequality and using (2.3) and (2.5), we obtain the upper bound

$$\|(\sigma-\sigma_h)\mathbf{n}\|_{0;\Gamma} \le C\left(\|\sigma\mathbf{n}-\pi_h^k(\sigma\mathbf{n})\|_{0;\Gamma} + \frac{1}{\sqrt{h}}\|\sigma - I_h^k\sigma\|_{0;S_h} + \frac{1}{\sqrt{h}}\|\sigma-\sigma_h\|_{0;S_h}\right).$$

The first two terms on the right yield, due to the best approximation property of $\pi_h^k$ and the local character of $I_h^k$, order $h^{k+1}$ estimates provided that the solution is sufficiently smooth. More precisely, for the second term, we can apply (2.6a) in combination with [15, Lemma 2.1].
The first term can be bounded in terms of (2.6b) and the fact that the trace operator is a bounded linear operator $B_{2,1}^{1/2}(\Omega) \to L^2(\Gamma)$, [22, Thm. 2.9.3]. ◻
Lemma 2.1 shows that there is some hope to recover an extra factor of $\sqrt{h}$ in the *a priori* estimates for the normal flux at the interface. We point out that this factor can be trivially found if the regularity is such that $L^\infty$-estimates of optimal order hold. We refer to [25] for $L^\infty$-estimates for mixed finite elements and note that these estimates require rather strong regularity assumptions. In the following theorem, which is the principal result of the paper, this assumption is considerably relaxed.
Theorem 2.2. *Let $\Omega \subset \mathbb{R}^d$, $d \in \{2,3\}$, be a convex polygon/polyhedron. Let $(\sigma, u) \in H(\mathrm{div};\Omega)\times L^2(\Omega)$ be the solution of the model problem (2.1) and let $(\sigma_h, u_h) \in V_h^k \times M_h^k$ be its finite element approximation, which satisfies (2.7). If $\sigma \in (B_{2,1}^{k+\frac{3}{2}}(\Omega))^d$, then the $L^2$-norm error of the flux on the interface $\Gamma$ can be bounded by*

$$\|(\sigma-\sigma_h)\mathbf{n}\|_{0;\Gamma} \le Ch^{k+1}|\log h|\|\sigma\|_{B_{2,1}^{k+\frac{3}{2}}}. \tag{2.9}$$

**3. Dual problems and their regularity.** The analysis of the $L^2$-error on the strip $S_h$, which is defined in (2.8), is based on a dual problem and closely related to the Aubin–Nitsche trick. However, we have to use suitable anisotropic norms and study the dual problem with right-hand sides supported by $S_h$.

**3.1. Dual problem formulation.** We denote by $(\lambda, w) \in H(\mathrm{div};\Omega) \times L^2(\Omega)$ the solution of the dual problem

$$a(\lambda,\tilde\sigma) + b(\tilde\sigma, w) = (\chi(\sigma-\sigma_h),\tilde\sigma)_0, \quad \tilde\sigma \in H(\mathrm{div};\Omega), \tag{3.1a}$$
$$b(\lambda,\tilde w) = 0, \quad \tilde w \in L^2(\Omega), \tag{3.1b}$$

where $0 \le \chi \le 1$ is a smooth cut-off function that is equal to one in $S_h$ and vanishes on $\{x \in \Omega\colon \mathrm{dist}(x,\Gamma) \ge \kappa h\}$ with $\kappa$ sufficiently large but independent on the mesh size. We will also assume

$$\|\nabla\chi/\sqrt{\chi}\|_{L^\infty} \le Ch^{-1}. \tag{3.2}$$

The mixed finite element solution of (3.1) is denoted by $(\lambda_h, w_h) \in V_h^k \times M_h^k$ and satisfies the Galerkin orthogonalities

$$a(\lambda-\lambda_h,\tilde\sigma_h) + b(\tilde\sigma_h, w-w_h) = 0, \quad \tilde\sigma_h \in V_h^k, \tag{3.3a}$$
$$b(\lambda-\lambda_h,\tilde u_h) = 0, \quad \tilde u_h \in M_h^k. \tag{3.3b}$$

It is well-known that a higher order *a priori* estimate can be obtained for the pressure, namely, using the convexity of $\Omega$, one can show (see, e.g., [7, outset of Sec. V.3])

$$\|w_h - \Pi_h^* w\|_0 \le Ch\|\lambda-\lambda_h\|_0. \tag{3.4}$$

Using $\lambda$ and $\lambda_h$ as test functions in (3.1a), (3.3a), and taking into account (3.1b), (3.3b), we get

$$\|\lambda\|_0 \le \|\chi(\sigma-\sigma_h)\|_0, \quad \|\lambda_h\|_0 \le \|\chi(\sigma-\sigma_h)\|_0. \tag{3.5}$$

For the further developments, it will be useful to note that for sufficiently regular $w$ we have

$$-\Delta w = \mathrm{div}(\chi(\sigma-\sigma_h)), \text{ on } \Omega, \qquad w = 0 \quad \text{on } \partial\Omega. \tag{3.6}$$

and correspondingly $\lambda = \chi(\sigma-\sigma_h) + \nabla w$.

**3.2. Regularity.** Our *a priori* analysis is based on regularity results of the solution $(\lambda, w)$ of (3.1). Let us study this problem in more generality by considering, for $g \in (L^2(\Omega))^d$, the problem of finding $(\lambda_g, w_g) \in H(\mathrm{div};\Omega) \times L^2(\Omega)$ such that

$$a(\lambda_g,\tilde\sigma) + b(\tilde\sigma, w_g) = (g,\tilde\sigma)_0, \qquad \tilde\sigma \in H(\mathrm{div};\Omega) \tag{3.7a}$$
$$b(\lambda_g,\tilde w) = 0, \qquad \tilde w \in L^2(\Omega). \tag{3.7b}$$

Let us denote by $T^M = (T_\lambda^M, T_w^M)$ the solution operator $g \mapsto (\lambda_g, w_g)$ for (3.7), i.e., $\lambda_g = T_\lambda^M g$ and $w_g = T_w^M g$. Then, the following two technical lemmas give us suitable regularity and stability results for the $w$-component $T_w^M g$.

Lemma 3.1. *Let $\Omega$ be a bounded Lipschitz domain. Then $T_w^M$ is a bounded linear operator with the following mapping properties:*

*(i) $T_w^M : (H(\mathrm{div};\Omega))' \to L^2(\Omega)$.*

*(ii)* $T_w^M : (L^2(\Omega))^d \to H_0^1(\Omega)$.
*(iii)* *If* $\Omega$ *is convex, then* $T_w^M : H(\mathrm{div};\Omega) \to H^2(\Omega) \cap H_0^1(\Omega)$.
*(iv)* *If* $\Omega$ *is convex, then* $T_w^M : \Big((B^{1/2}_{2,1}(\Omega))^d\Big)' \to B^{1/2}_{2,\infty}(\Omega)$.

*Proof.* The statement (i) follows from the well-posedness of the saddle point problem (3.7). To see (ii), let $\hat{w}_g \in H_0^1(\Omega)$ satisfy

$$(\nabla \hat{w}, \nabla \varphi)_0 = (g, \nabla\varphi)_0, \qquad \varphi \in H_0^1(\Omega) \tag{3.8}$$

and set $\hat{\lambda}_g := g - \nabla \hat{w}_g$. Then, we find $\operatorname{div} \hat{\lambda}_g = 0$ and thus $(\hat{\lambda}_g, \hat{w}_g) \in H(\mathrm{div};\Omega) \times L^2(\Omega)$. Moreover, $(\hat{\lambda}_g, \hat{w}_g)$ satisfies (3.7a) and (3.7b) are by definition and integration by parts. Since the solution of (3.7) is unique, we conclude $w_g = \hat{w}_g$; thus (ii) is valid. For $g \in H(\mathrm{div};\Omega)$, an integration by parts shows that $w_g$ not only solves (3.8) but also

$$(\nabla w_g, \nabla\varphi)_0 = -(\operatorname{div} g, \varphi)_0, \quad \varphi \in H_0^1(\Omega).$$

The standard shift-theorem for convex domains then gives $w \in H^2(\Omega)$ and thus (iii) holds.
Finally, we show (iv). The proof exploits an equivalence of the weak and the very weak formulation of Poisson problems in convex domains. We consider the variational problem: Find $y \in L^2(\Omega)$ such that

$$B(y,\varphi) := (y, \Delta\varphi)_0 = \langle g, \nabla\varphi\rangle_{((H^1(\Omega))^d)' \times (H^1(\Omega))^d}, \qquad \varphi \in H^2(\Omega)\cap H_0^1(\Omega), \tag{3.9}$$

where $\langle\cdot,\rangle_{((H^1(\Omega)))^d)'\times(H^1(\Omega))^d}$ stands for the duality pairing between $((H^1(\Omega))^d)'$ and $(H^1(\Omega)^d)$. By the convexity of $\Omega$, the bilinear form $B$ satisfies an inf-sup condition and thus the solution operator $T_{vw}^D : (H^1(\Omega))^d)' \to L^2(\Omega)$ given by $g \mapsto y$ is bounded and linear. Selecting $\varphi \in H^2(\Omega) \cap H_0^1(\Omega)$ in (3.8) and integrating by parts shows that $w_g$ also solves (3.9). By uniqueness, we thus get that the solution $y = T_{vw}^D g = w_g \in H_0^1(\Omega)$ if $g \in (L^2(\Omega))^d$. Having that $T_{vw}^D : (L^2(\Omega))^d \to H_0^1(\Omega) \subset H^1(\Omega)$ is bounded and linear, we can apply an interpolation argument to find that

$$T_{vw}^D : ((H^1(\Omega))^d)', (L^2(\Omega))^d)_{1/2,\infty} \to (L^2(\Omega), H^1(\Omega))_{1/2,\infty} = B^{1/2}_{2,\infty}(\Omega)$$

is bounded. Finally, we recall that $T_{vw}^D = T_w^M$ on $(L^2(\Omega))^d$ and note that, see, e.g., [22, Thm. 1.11.2] or [21, Lemma 41.3], we have

$$(((H^1(\Omega))^d)', (L^2(\Omega))^d)_{1/2,\infty} = \big((H^1(\Omega))^d, (L^2(\Omega))^d)_{1/2,1}\big)' = (B^{1/2}_{2,1}(\Omega))^d)'.$$

□

REMARK 3.2. *The assumption of convexity of* $\Omega$ *in assertion (iv) of Lemma 3.1 can be weakened: it suffices that* $\Omega$ *admit a shift theorem by more than* $1/2$*; see Appendix A for details.*

Next, we provide stability results in weighted Sobolev norms. As weight, we introduce the regularized distance $\delta$ from $\Gamma$, namely,

$$\delta(x) := h + \operatorname{dist}(x, \Gamma). \tag{3.10}$$

LEMMA 3.3. *Let the bounded Lipschitz domain* $\Omega \subset \mathbb{R}^d$*,* $d \in \{2,3\}$*, be a polygon (*$d = 2$*) or a polyhedron (*$d = 3$*). Then there exist* $c_1 \geq 1$*,* $c_2 > 0$ *independent of* $h$

*such that the following is true: if* $y \in B^{1/2}_{2,\infty}(\Omega)$ *solves* $-\Delta y = 0$ *in* $\Omega \setminus S_{c_1 h}$*, then*

$$\|\sqrt{\delta}\nabla y\|_{0;\Omega\setminus S_{c_2 h}} \le C\sqrt{|\log h|}\|y\|_{B^{1/2}_{2,\infty}(\Omega)}, \tag{3.11a}$$

$$\|\sqrt{\delta}\nabla^2 y\|_{0;\Omega\setminus S_{c_2 h}} \le C\sqrt{|\log h|}\|y\|_{B^{3/2}_{2,\infty}(\Omega)}, \quad \text{if } y \text{ in } B^{3/2}_{2,\infty}(\Omega). \tag{3.11b}$$

*Here,* $S_{\alpha h} := \{x \in \Omega,\ \mathrm{dist}(x, \Gamma) < \alpha h\}$.

*Proof.* The proof of (3.11b) can be found in [16, Lemma 5.4] and the proof of (3.11a) follows by the same type of arguments. ◻

We are now in a position to apply Lemma 3.1 and Lemma 3.3 to the dual problem (3.1), i.e., we set $g = \chi(\sigma - \sigma_h)$ in (3.7).

Lemma 3.4. *Let* $\Omega$ *be convex,* $(\lambda, w) \in H(\mathrm{div};\Omega) \times L^2(\Omega)$ *be the solution of (3.1). Then* $w \in H^2(\Omega) \cap H^1_0(\Omega)$*, and it satisfies*

$$\|\sqrt{\delta}\nabla w\|_0 \le C\sqrt{h}\sqrt{|\log h|}\|\chi(\sigma - \sigma_h)\|_0, \tag{3.12a}$$

$$\|\sqrt{\delta}\nabla^2 w\|_0 \le C\sqrt{h}\sqrt{|\log h|}\|\,\mathrm{div}(\chi(\sigma - \sigma_h))\|_0. \tag{3.12b}$$

*Proof.* We note that the support properties of $\chi$ imply that $w$ is harmonic in $\Omega \setminus S_{c_1 h}$ for suitably large $c_1 \ge 1$ and thus we are in the setting of Lemma 3.3. We start with the bound (3.12a) and decompose the domain $\Omega$ into $\Omega \setminus S_{c_2 h}$ and $S_{c_2 h}$. Then assertion (iv) of Lemma 3.1 in combination with [15, Lemma 2.1] yields

$$\|\sqrt{\delta}\nabla w\|_{0;\Omega\setminus S_{c_2 h}} \le C\sqrt{|\log h|}\|\chi(\sigma - \sigma_h)\|_{((B^{1/2}_{2,1}(\Omega))^d)'} \le C\sqrt{h}\|\chi(\sigma - \sigma_h)\|_0.$$

The assertion (ii) of Lemma 3.1 implies the bound $\|\nabla w\|_0 \le C\|\chi(\sigma - \sigma_h)\|_0$, and thus we have $\|\sqrt{\delta}\nabla w\|_{0;S_{c_2 h}} \le C\sqrt{h}\|\chi(\sigma - \sigma_h)\|_0$.

Proceeding as in the proof of (3.12a), we get in view of the assertion (iii) of Lemma 3.1

$$\|\sqrt{\delta}\nabla^2 w\|_{0;S_{c_2 h}} \le C\sqrt{h}\|\nabla^2 w\|_0 \le C\sqrt{h}\|\,\mathrm{div}(\chi(\sigma - \sigma_h))\|_0.$$

We note that [16, Lemma 5.2] and [15, Lemma 2.1] results in

$$\|w\|_{B^{3/2}_{2,\infty}(\Omega)} \le C\|\,\mathrm{div}(\chi(\sigma - \sigma_h))\|_{(B^{1/2}_{2,1}(\Omega))'} \le C\sqrt{h}\|\,\mathrm{div}(\chi(\sigma - \sigma_h))\|_0.$$

To bound the weighted norm on $\Omega \setminus S_{c_2 h}$, we use (3.11b)

$$\|\sqrt{\delta}\nabla^2 w\|_{0;\Omega\setminus S_{ch}} \le C\sqrt{|\log h|}\|w\|_{B^{3/2}_{2,\infty}(\Omega)} \le C\sqrt{|\log h|}\sqrt{h}\|\,\mathrm{div}(\chi(\sigma - \sigma_h))\|_0.$$

◻

## 4. Approximation in anisotropic norms.

In this section, we introduce anisotropic norms and reconsider the approximation properties of the Fortin operator $I^k_h$ and the $L^2$-projection $\Pi^*_h$ with respect to these norms.

### 4.1. Anisotropic norms.

The definition of our anisotropic norms is based on the decomposition of a $d$-dimensional domain into a one-dimensional and a $(d-1)$-dimensional subset and is closely related to weighted Sobolev spaces where the weight depends on the distance to $\Gamma$. Let us introduce the $(d-1)$-dimensional manifold $\gamma_\tau$ by

$$\gamma_\tau := \{x \in \Omega,\ \mathrm{dist}\ (x, \Gamma) = \tau\}, \quad \tau \ge 0.$$

We note that there exists a $D < \infty$ depending only on the diameter of $\Omega$ such that $\gamma_\tau = \emptyset$ for $\tau > D$. We place ourselves in the setting of the Fubini–Tonelli formula for integration over $\Omega$ and assume the existence of a measure $d\mu^\tau$ such that

$$\int_\Omega w dx = \int_{\tau=0}^D \int_{\gamma_\tau} w d\mu^\tau d\tau.$$

This is done for simplicity of exposition—in the general case, we can use a localization technique and fitted coordinate systems as done in [16].
Next, we introduce our anisotropic norms by

$$\|v\|_{L(p;2)} := \|v\|_{L^p((0,D);L^2(\gamma_\tau))} := \left( \int_{\tau=0}^D \left( \int_{\gamma_\tau} v^2 d\mu^\tau \right)^{\frac{p}{2}} d\tau \right)^{\frac{1}{p}}, \quad 1 \le p < \infty, \tag{4.1a}$$

$$\|v\|_{L(\infty;2)} := \|v\|_{L^\infty((0,D);L^2(\gamma_\tau))} := \sup_{\tau \in (0,D)} \left( \int_{\gamma_\tau} v^2 d\mu^\tau \right)^{\frac{1}{2}} \tag{4.1b}$$

and observe that for $p = 2$ we recover the standard $L^2(\Omega)$-norm. Roughly speaking the $L(p,2)$-norm has a $(d-1)$-dimensional $L^2$-component and a one-dimensional $L^p$-part. As a consequence of the one-dimensional Hölder inequality, we find

$$\left| \int_\Omega v\tilde{v}\ dx \right| \le \|v\|_{L(p;2)} \|\tilde{v}\|_{L(q;2)}, \quad \frac{1}{p} + \frac{1}{q} = 1. \tag{4.2}$$

**4.2. Approximation in anisotropic norms.** In this section, we reconsider the Fortin operator and its approximation properties with respect to our newly defined anisotropic norms. The definition (4.1b) of the $L(\infty;2)$-norm shows that we have to consider the $L^2(\gamma_\tau)$-norm in more detail. As a preliminary step, we introduce the sets

$$\overline{S}_h(\tau) := \cup_{T \in \mathcal{T}_\tau} \overline{T}, \quad \mathcal{T}_\tau := \{T \in \mathcal{T}_h \colon \gamma_\tau \cap \overline{T} \neq \emptyset\} \tag{4.3}$$

and observe that $S_h(\tau)$ is a subset of a strip of width $\mathcal{O}(h)$ around $\Gamma$.
LEMMA 4.1. *For $\sigma \in (B_{2,1}^{k+\frac{3}{2}}(\Omega))^d$, we have*

$$\|\sigma - I_h^k \sigma\|_{L(\infty;2)} \le Ch^{k+1} \|\sigma\|_{B_{2,1}^{k+\frac{3}{2}}}, \tag{4.4a}$$

$$\|\operatorname{div} \sigma - \Pi_h^* \operatorname{div} \sigma\|_{L(\infty;2)} \le Ch^k \|\operatorname{div} \sigma\|_{B_{2,1}^{k+\frac{1}{2}}}. \tag{4.4b}$$

*Proof.* Recalling (4.1b), we see that we have to bound the $L^2(\gamma_\tau)$-norm. The trace inequality in combination with the $H^1$-stability yields an upper bound for $\|\sigma - I_h^k\sigma\|_{0;\gamma_\tau}$ in terms of the norm restricted to $S_h(\tau)$. Due to (2.6a), we get

$$\begin{aligned}
\|\sigma - I_h^k \sigma\|_{0;\gamma_\tau}^2 &= \sum_{T \in \mathcal{T}_\tau} \|\sigma - I_h^k \sigma\|_{0;\gamma_\tau \cap \overline{T}}^2 \\
&\le C \sum_{T \in \mathcal{T}_\tau} \left( \frac{1}{h} \|\sigma - I_h^k \sigma\|_{0;T}^2 + h \|\nabla(\sigma - I_h^k \sigma)\|_{0;T}^2 \right) \\
&\le C \sum_{T \in \mathcal{T}_\tau} h^{2k+1} |\sigma|_{k+1;T}^2 \le Ch^{2k+1} |\sigma|_{k+1;S_h(\tau)}^2.
\end{aligned}$$

The definition (4.3) guarantees that an additional factor of $h$ can be recovered using [15, Lemma 2.1], i.e., $|\sigma|^2_{k+1;S_h(\tau)} \le Ch\|\sigma\|^2_{B^{k+\frac{3}{2}}_{2,1}}$ and thus (4.1b) yields (4.4a).

Now, we focus on (4.4b) and proceed as before

$$\begin{aligned}\|\operatorname{div}\sigma - \Pi_h^*\operatorname{div}\sigma\|^2_{0;\gamma_\tau} &= \sum_{T\in\mathcal{T}_\tau} \|\operatorname{div}\sigma - \Pi_h^*\operatorname{div}\sigma\|^2_{0;\gamma_\tau\cap\overline{T}} \\ &\le C\sum_{T\in\mathcal{T}_\tau}\left(\frac{1}{h}\|\operatorname{div}\sigma - \Pi_h^*\operatorname{div}\sigma\|^2_{0;T} + h\|\nabla(\operatorname{div}\sigma - \Pi_h^*\operatorname{div}\sigma)\|^2_{0;T}\right) \\ &\le C\sum_{T\in\mathcal{T}_\tau} h^{2k-1}|\operatorname{div}\sigma|^2_{k;T} \le Ch^{2k-1}|\operatorname{div}\sigma|^2_{k;S_h(\tau)} \le Ch^{2k}\|\operatorname{div}\sigma\|^2_{B^{k+\frac{1}{2}}_{2,1}}.\end{aligned}$$

□

REMARK 4.2. *We note that Lemma 4.1 is not sharp in the case that* $V_h^k = RT_h^k$. *Then* $k$ *on the right-hand side of* (4.4b) *can be replaced by* $k+1$ *provided that the solution is regular enough. However, this sharper result does not significantly improve the global estimate for the normal flux on the interface and is thus not stated.*

## 5. Proof of the main result.

In this section, we provide the proof of Theorem 2.2. To start with, we consider in Subsection 5.1 local $L^2$-estimate for the error $\sigma - \sigma_h$. In Subsection 5.2, we focus on *a priori* bounds for the error in the flux of the dual problem. Finally in Subsection 5.3, the main result (2.9) is established.

### 5.1. Local $L^2$-estimates.

The Aubin–Nitsche trick in combination with the Hölder type inequality (4.2) allows us to bound $\|\sqrt{\chi}(\sigma - \sigma_h)\|_0$.

LEMMA 5.1. *Let* $(\sigma, u) \in H(\operatorname{div};\Omega)\times L^2(\Omega)$ *be the solution of* (2.1) *and* $(\sigma_h, u_h) \in V_h^k \times M_h^k$ *be its finite element approximation. Let* $(\lambda, w) \in H(\operatorname{div};\Omega)\times L^2(\Omega)$ *be the solution of the dual problem* (3.1) *and* $(\lambda_h, w_h) \in V_h^k\times M_h^k$ *be its finite element approximation. Then for* $\sigma \in B^{k+\frac{3}{2}}_{2,1}(\Omega)$, *we have*

$$\|\sqrt{\chi}(\sigma - \sigma_h)\|_0^2 \le Ch^k\left(h\|\lambda - \lambda_h\|_{L(1;2)} + \|w - \Pi_h^* w\|_{L(1;2)}\right)\|\sigma\|_{B^{k+\frac{3}{2}}_{2,1}}. \tag{5.1}$$

*Proof.* A crucial observation for the proof is that $\operatorname{div}\lambda_h = 0$. This follows from the fact that $\operatorname{div} V_h^k = M_h^k$ and (3.1b), (3.3b). Moreover, we recall that by (2.1b), we have $b(\sigma - \sigma_h, v_h) = 0$ for all $v_h \in M_h^k$. The symmetry of the bilinear form $a(\cdot,\cdot)$ yields in combination with (2.1a) that $a(\tau_h, \sigma - \sigma_h) = 0$ for all $\tau_h \in V_h$ with $\operatorname{div}\tau_h = 0$. Using the definition of the dual solution and exploiting the Galerkin orthogonality (2.7a), we find

$$\begin{aligned}\|\sqrt{\chi}(\sigma - \sigma_h)\|_0^2 &= (\chi(\sigma - \sigma_h), \sigma - \sigma_h)_0 = a(\lambda, \sigma - \sigma_h) + b(\sigma - \sigma_h, w) \\ &= a(\lambda - \lambda_h, \sigma - \sigma_h) + b(\sigma - \sigma_h, w - w_h).\end{aligned}$$

Now using the Galerkin orthogonality (3.3a), we can replace the finite element solution $\sigma_h$ by the Fortin interpolation of $\sigma$ and $w_h$ by the $L^2$-projection of $w$

$$\begin{aligned}\|\sqrt{\chi}(\sigma - \sigma_h)\|_0^2 &= a(\lambda - \lambda_h, \sigma - I_h^k\sigma) + b(\sigma - I_h^k\sigma, w - w_h) \\ &= a(\lambda - \lambda_h, \sigma - I_h^k\sigma) + b(\sigma - I_h^k\sigma, w - \Pi_h^* w).\end{aligned}$$

The Hölder type inequality (4.2) for our anisotropic norms yields

$$\begin{aligned}\|\sqrt{\chi}(\sigma - \sigma_h)\|_0^2 \le\ & \|\lambda - \lambda_h\|_{L(1;2)}\|\sigma - I_h^k\sigma\|_{L(\infty;2)} \\ &+ \|w - \Pi_h^* w\|_{L(1;2)}\|\operatorname{div}\sigma - \Pi_h^*(\operatorname{div}\sigma)\|_{L(\infty;2)}.\end{aligned}$$

To obtain a bound for $\|\sqrt{\chi}(\sigma - \sigma_h)\|_0^2$ in terms of the mesh size, we have to control the terms on the right-hand side. The two terms associated with the solution $\sigma$ and the Fortin interpolant $I_h^k\sigma$ are covered by Lemma 4.1. For $\sigma \in B_{2,1}^{k+\frac{3}{2}}(\Omega)$, we have $\|\operatorname{div}\sigma\|_{B_{2,1}^{k+\frac{1}{2}}} \leq \|\sigma\|_{B_{2,1}^{k+\frac{3}{2}}}$ and thus (4.4a) in combination with (4.4b) gives (5.1). □

**5.2. A priori bounds on the error in the dual flux.** The estimate for $\sigma - \sigma_h$ in Lemma 5.1 involves anisotropic norms of the FEM-error $\lambda - \lambda_h$ and the approximation error $w - \Pi_h^* w$ for the solution $(\lambda, w)$ of the dual problem (3.1). In this subsection, we focus on the error in the flux variable $\lambda$ and use the regularity assertions for $w$ given in Lemma 3.4.

We start with some preliminary technical results which play an important role in the bound for the flux error. As is standard for localized estimates in the context of finite element approximation, we have to use a "super approximation" property (see, e.g., [23, 24] for its use in Poisson-type problem and also [8] for its use in the context of mixed finite elements).

LEMMA 5.2 ("super approximation"). *Fix $T \in \mathcal{T}_h$. Let $z \in W^{1;\infty}(T)$ be such that $\|\nabla z\|_{W^{0;\infty}(T)} \leq C_z h^{-1}\|z\|_{W^{0;\infty}(T)}$. Then there exists a constant $C > 0$ depending only on the shape regularity of $T$, the constant $C_z$ and $k$ such that*

$$\|z\tau_h - I_h^k(z\tau_h)\|_{0;T} \leq Ch\|\nabla z\|_{W^{0;\infty}(T)}\|\tau_h\|_{0;T}, \quad \tau_h \in V_k(T), \tag{5.2a}$$

$$\|I_h^k(z\tau_h)\|_{0;T} \leq C\|z\|_{W^{0;\infty}(T)}\|\tau_h\|_{0;T}, \quad \tau_h \in V_k(T). \tag{5.2b}$$

*Proof.* We start with the stability bound (5.2b). Since the Fortin operator is not $H(\operatorname{div};T)$-stable, we use the triangle inequality, an inverse estimate for polynomials and the approximation property (2.6a) to find

$$\begin{aligned}\|I_h^k(z\tau_h)\|_{0;T} &\leq \|z\tau_h - I_h^k(z\tau_h)\|_{0;T} + \|z\tau_h\|_{0;T} \\ &\leq C\left(h|z\tau_h|_{1;T} + \|z\tau_h\|_{0;T}\right) \\ &\leq C\left(h\|z\|_{W^{1;\infty}(T)}\|\tau_h\|_{0;T} + \|z\|_{W^{0;\infty}(T)}\|\tau_h\|_{0;T}\right) \leq C\|z\|_{W^{0;\infty}(T)}\|\tau_h\|_{0;T}.\end{aligned}$$

Now, (5.2a) can easily be shown using (5.2b). Recalling that $\Pi_h^0 z|_T\tau_h \in V_k(T)$ and that the definition of $I_h^k(z\tau_h)$ only involves values of $z\tau_h$ restricted to $T$, we get

$$\begin{aligned}\|z\tau_h - I_h^k(z\tau_h)\|_{0;T} &= \|(z - \Pi_h^0 z)\tau_h - I_h^k((z - \Pi_h^0 z)\tau_h)\|_{0;T} \\ &\leq C\|z - \Pi_h^0 z\|_{W^{0;\infty}(T)}\|\tau_h\|_{0;T} \leq Ch\|\nabla z\|_{W^{0;\infty}(T)}\|\tau_h\|_{0;T}.\end{aligned}$$

□

The proof of the following Lemma 5.3 requires the introduction of some notation. For $x \in \Omega$ we select two balls $\tilde{B}_{\delta;x}^i$, $i \in \{1,2\}$ centered at $x$ with radii $\kappa_i\delta(x)$, where $0 < \kappa_1 < \kappa_2$ are chosen independent of the mesh size suitably so that certain covering arguments can be carried out below. We set $B_{\delta;x}^i := \tilde{B}_{\delta;x}^i \cap \Omega$. Furthermore, we select $\chi_x \in W^{1;\infty}(\Omega)$ with $\operatorname{supp} chi_x \subset B_{\delta;x}^2$ and $\chi_x \equiv 1$ on $B_{\delta;x}^1$. Furthermore, we require $\|\nabla\chi_x/\sqrt{\chi_x}\|_{W^{0;\infty}} \leq C\delta(x)^{-1}$. Then we obtain with the aid of the local super approximation property (5.2a) and the bound on the gradient of $\chi_x$ the estimate

$$\|\chi_x\tau_h - I_h^k(\chi_x\tau_h)\|_0 \leq C\frac{h}{\delta(x)}\|\tau_h\|_{0;B_{\delta;x}^2}, \quad \tau_h \in V_h^k. \tag{5.3}$$

To apply the regularity results of Section 3, we relate our anisotropic $L(1;2)$-norm with a weighted $L^2$-norm. It can easily be shown by decomposing the interval $(0, D)$

into the two sub-intervals $(0,h)$ and $(h,D)$ that

$$\begin{aligned}\|v\|_{L(1;2)} &= \int_{\tau=0}^{h}\left(\int_{\gamma_\tau} v^2 d\mu^\tau\right)^{\frac{1}{2}} d\tau + \int_{\tau=h}^{D}\left(\int_{\gamma_\tau} v^2 d\mu^\tau\right)^{\frac{1}{2}} d\tau \\ &\le \sqrt{h}\|v\|_{0;S_h} + \left(\int_{\tau=h}^{D} \tau^{-1}\, d\tau \int_{\tau=h}^{D}\int_{\gamma_\tau} \tau v^2\, dx\, d\tau\right)^{1/2} \\ &\le \sqrt{h}\|v\|_{0;S_h} + C|\log h|^{\frac{1}{2}}\|\sqrt{\delta} v\|_{0;\Omega\setminus S_h}. \qquad (5.4)\end{aligned}$$

LEMMA 5.3. *Let $(\sigma,u) \in H(\mathrm{div};\Omega)\times L^2(\Omega)$ be the solution of (2.1) and $(\sigma_h,u_h) \in V_h^k \times M_h^k$ be its finite element approximation. Let $(\lambda,w) \in H(\mathrm{div};\Omega)\times L^2(\Omega)$ be the solution of the dual problem (3.1) and $(\lambda_h,w_h) \in V_h^k \times M_h^k$ be its finite element approximation. Then, we have the bound*

$$\|\lambda-\lambda_h\|_{L(1;2)}^2 \le Ch\,|\log h|\left(\|\chi(\sigma-\sigma_h)\|_0^2 + h^2\,|\log h|\|\operatorname{div}(\chi(\sigma-\sigma_h))\|_0^2\right).$$

*Proof.* In view of (5.4), we estimate $\|\lambda-\lambda_h\|_{0;S_{ch}}$ and $\|\sqrt{\delta}(\lambda-\lambda_h)\|_{0;\Omega\setminus S_{ch}}$ separately for $c \ge 1$ sufficiently large. The stability estimates (3.5) readily give $\sqrt{h}\|\lambda-\lambda_h\|_{0;S_{ch}} \le 2\sqrt{h}\|\chi(\sigma-\sigma_h)\|_0$, which is stronger than required.
For the treatment of $\|\sqrt{\delta}(\lambda-\lambda_h)\|_{0;\Omega\setminus S_{ch}}$, we assume that $c \ge 1$ so large that $w$ is harmonic on $\Omega \setminus S_{2ch}$. We fix $x \in \Omega$. We start by considering the $L^2$-norm of $\lambda-\lambda_h$ restricted to $B^1_{\delta;x}$. Using the super approximation property (5.3), (3.1a) and the fact that $\delta(x) \ge h$, we find

$$\begin{aligned}\|\lambda-\lambda_h\|^2_{0;B^1_{\delta;x}} &\le (\chi_x(\lambda-\lambda_h),\lambda-\lambda_h)_0 \\ &= (\chi_x(\lambda-I_h^k\lambda),\lambda-\lambda_h)_0 + (\chi_x(I_h^k\lambda-\lambda_h),\lambda-\lambda_h)_0 \\ &\le C\|\lambda-\lambda_h\|_{0;B^2_{\delta;x}}\left(\|\lambda-I_h^k\lambda\|_{0;B^2_{\delta;x}} + \frac{h}{\delta(x)}\|\lambda_h-I_h^k\lambda\|_{0;B^2_{\delta;x}}\right) \\ &\quad + b(I_h^k(\chi_x(I_h^k\lambda-\lambda_h)),w_h-w) \\ &\le C\|\lambda-\lambda_h\|_{0;B^2_{\delta;x}}\left(\|\lambda-I_h^k\lambda\|_{0;B^2_{\delta;x}} + \frac{h}{\delta(x)}\|\lambda_h-\lambda\|_{0;B^2_{\delta;x}}\right) \\ &\quad + b(I_h^k(\chi_x(I_h^k\lambda-\lambda_h)),w_h-\Pi_h^* w). \qquad (5.5)\end{aligned}$$

To estimate the contribution from the bilinear form $b(\cdot,\cdot)$ we use the properties (2.4a), (2.4b), the product rule, and the fact that $I_h^k\lambda$ and $\lambda_h$ are divergence free to get

$$\begin{aligned}b(I_h^k(\chi_x(I_h^k\lambda-\lambda_h)),w_h-\Pi_h^*w) &= b(\chi_x(I_h^k\lambda-\lambda_h),w_h-\Pi_h^*w) \\ &\le \|\operatorname{div}(\chi_x(I_h^k\lambda-\lambda_h))\|_0\|w_h-\Pi_h^*w\|_{0;B^2_{\delta;x}} \\ &\le \frac{C}{\delta(x)}\|I_h^k\lambda-\lambda_h\|_{0;B^2_{\delta;x}}\|w_h-\Pi_h^*w\|_{0;B^2_{\delta;x}}. \qquad (5.6)\end{aligned}$$

Next, we consider a countable, locally finite covering of $\Omega\setminus S_{2ch}$ by balls $\{B^1_{\delta;x_i} : i \in \mathbb{N}\}$ such that the associated covering $\{B^2_{\delta;x_i} : i \in \mathbb{N}\}$ is also locally finite; for details for the construction we refer to [16, Appendix]. We assume furthermore that the sets $B^2_{\delta;x_i}$, $i \in \mathbb{N}$, are contained in $\Omega \setminus S_{ch}$. We note that for each $y \in B^j_{\delta;x_i}$ we have equivalence of $\delta(y)$ and $\delta(x)$.

Applying Young's inequality for $\epsilon > 0$, we get using (5.5), (5.6), and exploiting the observation $\lambda = -\nabla w$ on $\Omega \setminus S_{ch}$

$$\|\sqrt{\delta}(\lambda - \lambda_h)\|_0^2 \le C \sum_{x_i} \delta(x_i) \|\lambda - \lambda_h\|^2_{0;B^1_{\delta;x_i}}$$
$$\le C \sum_{x_i} \left( \delta(x_i) \|\lambda - I_h^k \lambda\|_{0;B^2_{\delta;x_i}} \|\lambda - \lambda_h\|_{0;B^2_{\delta;x_i}} + h \|\lambda_h - \lambda\|^2_{0;B^2_{\delta;x_i}} \right)$$
$$+ C \sum_{x_i} \frac{1}{\sqrt{h}} \|w_h - \Pi_h^* w\|_{0;B^2_{\delta;x_i}} \sqrt{h} \|I_h^k \lambda - \lambda_h\|_{0;B^2_{\delta;x_i}}$$
$$\le C \left( (\frac{1}{\epsilon} + 1) \|\sqrt{\delta}(\lambda - I_h^k \lambda)\|_0^2 + \epsilon \|\sqrt{\delta}(\lambda - \lambda_h)\|_0^2 + h \|\lambda_h - \lambda\|_0^2 + \frac{1}{h} \|w_h - \Pi_h^* w\|_0^2 \right).$$

For $\epsilon > 0$ fixed but small enough, we get by (2.6a) and $s = 0$

$$\|\sqrt{\delta}(\lambda - \lambda_h)\|_0^2 \le C \left( h^2 \|\sqrt{\delta} \nabla \lambda\|_0^2 + h \|\lambda_h - \lambda\|_0^2 + \frac{1}{h} \|w_h - \Pi_h^* w\|_0^2 \right)$$
$$\le C \left( h^2 \|\sqrt{\delta} \nabla^2 w\|_0^2 + h \|\chi(\sigma - \sigma_h)\|_0^2 + h \|\lambda_h - \lambda\|_0^2 + \frac{1}{h} \|w_h - \Pi_h^* w\|_0^2 \right)$$
$$\le C \left( h^2 \|\sqrt{\delta} \nabla^2 w\|_0^2 + h \|\chi(\sigma - \sigma_h)\|_0^2 \right).$$

In the two last steps, we have used the super approximation property (3.4) of $w_h$ with respect to $\Pi_h^* w$ and the stability (3.5) of $\lambda$ and $\lambda_h$. To bound $\|\sqrt{\delta} \nabla^2 w\|_0$, we use (3.12b). □

**5.3. Proof of the main result.** In this subsection, we show that Theorem 2.2 holds. The starting point of the proof is Lemma 5.1. Using (5.4) in combination with (3.12a), we get

$$\|w - \Pi_h^* w\|^2_{L(1;2)} \le C h^2 |\log h| \|\sqrt{\delta} \nabla w\|_0^2 \le C h^3 |\log h|^2 \|\chi(\sigma - \sigma)\|_0^2. \tag{5.7}$$

Inserting the result of Lemma 5.3 and the bound (5.7) into Lemma 5.1 we find

$$\|\sqrt{\chi}(\sigma - \sigma_h)\|_0^4 \le C h^{2k+3} |\log h|^2 \|\sigma\|^2_{B^{k+\frac{3}{2}}_{2,1}} \left( \|\chi(\sigma - \sigma_h)\|_0^2 + h^2 \|\operatorname{div}(\chi(\sigma - \sigma_h))\|_0^2 \right).$$

We recall that $\operatorname{div}(\chi(\sigma - \sigma_h)) = \nabla \chi \cdot (\sigma - \sigma_h) + \chi \operatorname{div}(\sigma - \sigma_h)$ and thus we get in view of (3.2)

$$\|\operatorname{div}(\chi(\sigma - \sigma_h))\|_0^2 \le C \left( \frac{1}{h^2} \|\sqrt{\chi}(\sigma - \sigma_h)\|_0^2 + \|\chi(\operatorname{div} \sigma - \Pi_h^* \operatorname{div} \sigma)\|_0^2 \right)$$
$$\le C \left( \frac{1}{h^2} \|\sqrt{\chi}(\sigma - \sigma_h)\|_0^2 + h^{2k+1} \|\sigma\|^2_{B^{k+\frac{3}{2}}_{2,1}} \right).$$

Finally this bound results in

$$\|\sqrt{\chi}(\sigma - \sigma_h)\|_0^4 \le C h^{2k+3} |\log h|^2 \|\sigma\|^2_{B^{k+\frac{3}{2}}_{2,1}} \left( \|\sqrt{\chi}(\sigma - \sigma_h)\|_0^2 + h^{2k+3} \|\sigma\|^2_{B^{k+\frac{3}{2}}_{2,1}} \right)$$

and thus $\|(\sigma - \sigma_h)\|_{0;S_h} \le \|\sqrt{\chi}(\sigma - \sigma_h)\|_0 \le C h^{k+3/2} |\log h| \|\sigma\|_{B^{k+\frac{3}{2}}_{2,1}}$. Now, our main result, the *a priori* bound (2.9), follows from Lemma 2.1.

**6. Numerical results.** In this section, we present two examples to confirm the theoretical convergence rates for the Laplace operator and one example with an application to the Stokes–Darcy coupling. In all three examples, we consider problem settings with a given solution on $\Omega \subset \mathbb{R}^2$. Beside the finite elements on triangles, which we introduced in Section 2.1, we also consider finite elements on quadrilaterals such as $RT_h^{[k]}$, $BDM_h^{[k]}$ and $BDFM_h^{[k]}$, $k \in \mathbb{N}_0$ (see Fig. 6.1). Following the notation of [7], the subscript $[\cdot]$ indicates the association to quadrilateral elements. Note that, unlike the triangular case, where we have that $RT_h^k \subset BDM_h^{k+1} \subset RT_h^{k+1}$, this relationship does not hold anymore for the quadrilateral case, since $\operatorname{div}(RT_h^{[k]}) = Q_k \not\subseteq P_k = \operatorname{div}(BDM_h^{[k+1]})$. Figure 6.1 illustrates the elements employed and shows the number of degrees of freedom associated with the edges and elements.

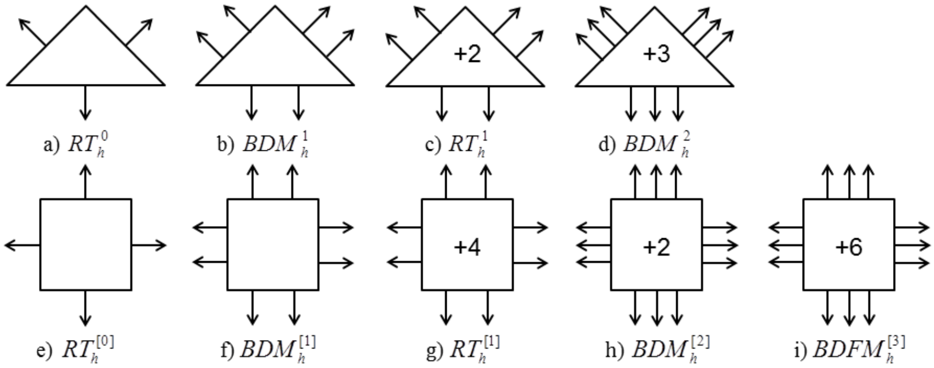


FIG. 6.1. *Degrees of freedom of RT- and BDM-elements on triangles and quadrilaterals*

**6.1. Two dimensional model problems.** Here, we consider two different types of examples. Firstly, we introduce on $\Omega = (0,1)^2$, the parameter-dependent exact solution by

$$u = r^\alpha \sin\phi, \quad r = \|(x,y)^T - (0.75, 0.5)^T\|,$$

where $\|\cdot\|$ denote the Euclidean distance. The interface $\Gamma$ is placed at $y = 0.5$ and resolved by the mesh. We focus on the choices $\alpha = 1.5$ and $\alpha = 1.75$. We note that for $\frac{3}{2} < \alpha < 2$, the solution is in $B_{2,1}^{3/2}(\Omega)$ but not in $W^{2,\infty}(\Omega)$, and that no full convergence rates can be expected due to the limited regularity.

**6.1.1. Simplicial mesh.** In Tables 6.1 and 6.2, the $L^2$-errors of the normal fluxes across the interface are presented for the limit case $\alpha = \frac{3}{2}$ and the case $\alpha = 1.75$ for various levels of uniform refinement. The domain is resolved by an unstructured simplicial mesh, and we use $RT_h^0, RT_h^1$, $BDM_h^1$ and $BDM_h^2$ elements. As expected from the theoretical point of view, the achieved asymptotic convergences rates are determined by the low regularity of the problem. We note that the singularity is not placed at a vertex of the initial mesh.

In Figures 6.2–6.3, the normal fluxes of the numerical solutions are plotted against that of the exact solution $u$ for both choices of $\alpha$. We point out that only for $RT_h^0$, the flux is approximated by a piecewise constant whereas for the cases $RT_h^1$ and $BDM_h^1$ the flux is approximated by linears and for $BDM_h^2$ by quadratics.

Table 6.1
*Error in the flux for $\alpha = 1.5$*

| level | $RT_h^0$ | rate | $BDM_h^1$ | rate | $RT_h^1$ | rate | $BDM_h^2$ | rate |
|---|---|---|---|---|---|---|---|---|
| 1 | 9.42e-2 | - | 4.84e-2 | - | 2.201e-2 | - | 1.75e-2 | - |
| 2 | 5.03e-2 | 0.904 | 2.48e-2 | 0.964 | 1.07e-2 | 1.040 | 8.76e-3 | 1.000 |
| 3 | 2.70e-2 | 0.896 | 1.24e-2 | 1.003 | 5.36e-3 | 1.003 | 4.37e-3 | 1.002 |
| 4 | 1.44e-2 | 0.905 | 6.19e-3 | 1.001 | 2.68e-3 | 1.001 | 2.19e-3 | 1.001 |
| 5 | 7.65e-3 | 0.916 | 3.09e-3 | 1.000 | 1.34e-3 | 1.001 | 1.09e-3 | 1.001 |
| 6 | 4.03e-3 | 0.925 | 1.55e-3 | 1.000 | 6.64e-4 | 1.000 | 5.45e-4 | 1.002 |

Table 6.2
*Error in the flux for $\alpha = 1.75$*

| level | $RT_h^0$ | rate | $BDM_h^1$ | rate | $RT_h^1$ | rate | $BDM_h^2$ | rate |
|---|---|---|---|---|---|---|---|---|
| 1 | 8.44e-2 | - | 3.36e-2 | - | 1.12e-2 | - | 8.35e-3 | - |
| 2 | 4.23e-2 | 0.996 | 1.44e-2 | 1.225 | 4.40e-3 | 1.349 | 3.51e-3 | 1.252 |
| 3 | 2.14e-2 | 0.985 | 5.92e-3 | 1.280 | 1.84e-3 | 1.257 | 1.48e-3 | 1.248 |
| 4 | 1.08e-2 | 0.987 | 2.46e-3 | 1.265 | 7.72e-4 | 1.252 | 6.21e-4 | 1.250 |
| 5 | 5.43e-3 | 0.990 | 1.03e-3 | 1.256 | 3.24e-4 | 1.252 | 2.61e-4 | 1.249 |
| 6 | 2.73e-3 | 0.993 | 4.33e-4 | 1.252 | 1.36e-4 | 1.257 | 1.10e-4 | 1.250 |

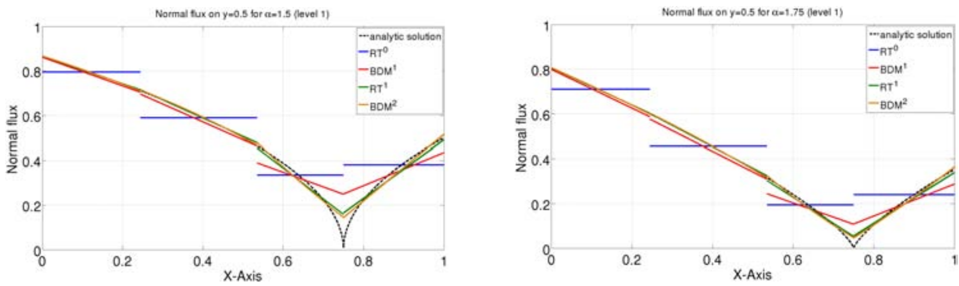


Fig. 6.2. *Numerical approximation of the normal flux across the interface $\Gamma$ for $\alpha = 1.5$ (left) and $\alpha = 1.75$ (right) on refinement level 1 (simplicial mesh)*

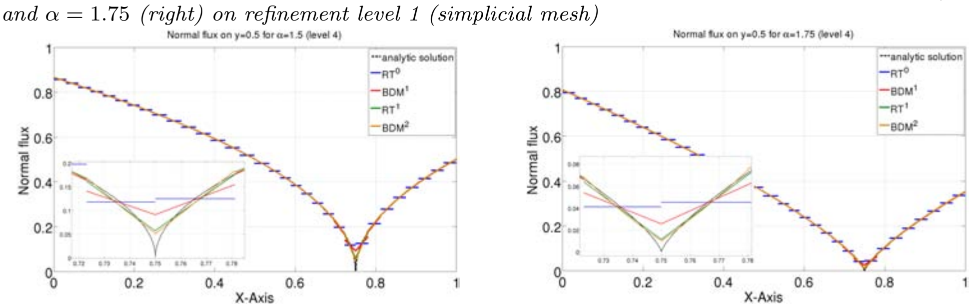


Fig. 6.3. *Numerical approximation of the normal flux across the interface $\Gamma$ for $\alpha = 1.5$ (left) and $\alpha = 1.75$ (right) on refinement level 4 (simplicial mesh)*

**6.1.2. Quadrilateral mesh.** Tables 6.3 and 6.4 show the same type of results but for mixed finite elements on a quadrilateral mesh, in particular for $RT_h^{[0]}$, $RT_h^{[1]}$, $BDM_h^{[1]}$, $BDM_h^{[2]}$ and $BDFM_h^{[3]}$ elements. In Table 6.3, the case $\alpha = 1.5$ is displayed. Here we cannot expect a higher convergence rate than one independently of the choice of the finite element order. We recall that $BDM_h^{[1]}$ and $RT_h^{[1]}$ have the same degrees of freedom per edge but $RT_h^{[1]}$ has additional interior degrees of freedom and thus has a significantly smaller error on all levels. Although $BDM_h^{[2]}$ and $BDFM_h^{[3]}$ have more degrees of freedom per edge than $RT_h^{[1]}$, the quantitative errors are sensitive to the number of degrees of freedom per element.

Table 6.3
*Error in the flux for $\alpha = 1.5$, quadrilateral mesh*

| level | $RT_h^{[0]}$ | rate | $BDM_h^{[1]}$ | rate | $RT_h^{[1]}$ | rate | $BDM_h^{[2]}$ | rate | $BDFM_h^{[3]}$ | rate |
|---|---|---|---|---|---|---|---|---|---|---|
| 0 | 1.18e-1 | - | 8.98e-2 | - | 8.41e-2 | - | 6.59e-2 | - | 5.28e-2 | - |
| 1 | 9.28e-2 | 0.348 | 5.97e-2 | 0.589 | 1.81e-2 | 2.218 | 3.40e-2 | 0.955 | 1.88e-2 | 1.486 |
| 2 | 5.14e-2 | 0.852 | 3.07e-2 | 0.956 | 8.73e-3 | 1.051 | 1.65e-2 | 1.038 | 9.45e-3 | 0.996 |
| 3 | 2.77e-2 | 0.890 | 1.54e-2 | 0.998 | 4.37e-3 | 0.999 | 8.28e-3 | 1.000 | 4.72e-3 | 1.000 |
| 4 | 1.48e-2 | 0.902 | 7.68e-3 | 1.004 | 2.18e-3 | 1.000 | 4.14e-3 | 1.000 | 2.36e-3 | 1.000 |
| 5 | 7.88e-3 | 0.913 | 3.84e-3 | 1.001 | 1.09e-3 | 1.000 | 2.07e-3 | 1.000 | 1.18e-3 | 1.000 |
| 6 | 4.16e-3 | 0.923 | 1.92e-3 | 1.000 | 5.46e-4 | 1.000 | 1.03e-3 | 1.000 | 5.91e-4 | 1.000 |

Table 6.4
*Error in the flux for $\alpha = 1.75$, quadrilateral mesh*

| level | $RT_h^{[0]}$ | rate | $BDM_h^{[1]}$ | rate | $RT_h^{[1]}$ | rate | $BDM_h^{[2]}$ | rate | $BDFM_h^{[3]}$ | rate |
|---|---|---|---|---|---|---|---|---|---|---|
| 0 | 1.21e-1 | - | 8.36e-2 | - | 6.82e-2 | - | 4.79e-2 | - | 3.55e-2 | - |
| 1 | 8.33e-2 | 0.540 | 4.41e-2 | 0.923 | 7.81e-3 | 3.125 | 2.07e-2 | 1.212 | 1.05e-2 | 1.758 |
| 2 | 4.29e-2 | 0.959 | 1.89e-2 | 1.222 | 2.92e-3 | 1.418 | 8.35e-3 | 1.307 | 4.44e-3 | 1.240 |
| 3 | 2.16e-2 | 0.986 | 7.83e-3 | 1.272 | 1.23e-3 | 1.247 | 3.52e-3 | 1.246 | 1.87e-3 | 1.250 |
| 4 | 1.09e-2 | 0.987 | 3.25e-3 | 1.267 | 5.21e-4 | 1.243 | 1.48e-3 | 1.249 | 7.85e-4 | 1.250 |
| 5 | 5.49e-3 | 0.990 | 1.36e-3 | 1.257 | 2.19e-4 | 1.249 | 6.23e-4 | 1.250 | 3.30e-4 | 1.250 |
| 6 | 2.76e-3 | 0.993 | 5.71e-4 | 1.253 | 9.26e-5 | 1.250 | 2.62e-4 | 1.250 | 1.39e-4 | 1.250 |

Compared to $\alpha = 1.5$, the solution for $\alpha = 1.75$ is more regular, and thus we only expect for the lowest order $RT_h^{[0]}/RT_h^0$ discretization an asymptotic rate of one. In all other cases, we observe asymptotically a rate of approximately 1.25. There is no qualitative difference between an unstructured simplicial mesh and a regular quadrilateral mesh.

**6.1.3. Higher order convergence.** In the second example, we consider the piecewise smooth solution

$$u = \begin{cases} e^{-x}\sin(2\pi y)^2 & -\left(y-\frac{1}{2}\right)\left[xy(x-\frac{1}{2})^2 + e^y\cos(8\pi xy)(x+\frac{1}{2})^2\right] \quad \text{if } y < \frac{1}{2} \\ e^{-x}(y-\frac{1}{2})^2 4\pi^2 & -\left(y-\frac{1}{2}\right)\left[xy(x-\frac{1}{2})^2 + e^y\cos(8\pi xy)(x+\frac{1}{2})^2\right] \quad \text{if } y \geq \frac{1}{2} \end{cases}.$$

on $\Omega = (0,1)^2$. The interface $\Gamma$ is placed at $y = 0.5$ and resolved by the mesh. Since the exact solution is sufficiently smooth we expect full convergence rates. Tables 6.5 and 6.6 show the numerical results for a uniform quadrilateral and a simplicial mesh, respectively. The observed convergence rates confirm our theoretical result. Note that the absolute errors for $BDM_h^{[2]}$ is again smaller than for $RT^{[1]}$ on the first four refinement levels although it has an additional degree of freedom per edge.

Table 6.5
*Error in the flux, quadrilateral mesh*

| level | $RT_h^{[0]}$ | rate | $BDM_h^{[1]}$ | rate | $RT_h^{[1]}$ | rate | $BDM_h^{[2]}$ | rate | $BDFM_h^{[3]}$ | rate |
|---|---|---|---|---|---|---|---|---|---|---|
| 1 | 1.69e-0 | - | 1.55e-0 | - | 1.10e-0 | - | 2.64e-0 | - | 1.49e-0 | - |
| 2 | 8.13e-1 | 1.053 | 8.45e-1 | 0.871 | 4.15e-1 | 1.408 | 7.49e-1 | 1.819 | 3.32e-1 | 2.167 |
| 3 | 4.08e-1 | 0.996 | 2.11e-1 | 2.004 | 4.83e-2 | 3.103 | 1.41e-1 | 2.414 | 2.43e-2 | 3.774 |
| 4 | 1.81e-1 | 1.168 | 6.51e-2 | 1.695 | 8.55e-3 | 2.499 | 1.86e-2 | 2.915 | 1.24e-3 | 4.291 |
| 5 | 8.51e-2 | 1.091 | 1.75e-2 | 1.890 | 2.08e-3 | 2.042 | 2.33e-3 | 3.001 | 7.11e-5 | 4.123 |
| 6 | 4.18e-2 | 1.027 | 4.53e-3 | 1.953 | 5.19e-4 | 2.001 | 2.91e-4 | 3.001 | 5.78e-6 | 3.622 |
| 7 | 2.08e-2 | 1.012 | 1.15e-3 | 1.979 | 5.19e-4 | 2.001 | 3.63e-5 | 3.000 | 6.16e-7 | 3.230 |

TABLE 6.6
*Error in the flux, simplicial mesh*

| level | $RT_h^0$ | rate | $BDM_h^1$ | rate | $RT_h^1$ | rate | $BDM_h^2$ | rate |
|---|---|---|---|---|---|---|---|---|
| 1 | 1.83e-0 | - | 1.67e-0 | - | 1.57e-0 | - | 1.90e-0 | - |
| 2 | 9.26e-1 | 0.987 | 8.35e-1 | 1.004 | 4.10e-1 | 1.934 | 2.83e-1 | 2.749 |
| 3 | 4.19e-1 | 1.145 | 2.26e-1 | 1.886 | 8.16e-2 | 2.329 | 5.32e-2 | 2.410 |
| 4 | 1.86e-1 | 1.173 | 5.45e-2 | 2.051 | 1.41e-2 | 2.534 | 7.42e-3 | 2.842 |
| 5 | 8.62e-2 | 1.108 | 1.33e-2 | 2.039 | 2.67e-3 | 2.398 | 9.54e-4 | 2.960 |
| 6 | 4.20e-2 | 1.038 | 3.33e-3 | 1.995 | 5.79e-4 | 2.206 | 1.20e-4 | 2.990 |
| 7 | 2.08e-2 | 1.010 | 8.38e-4 | 1.989 | 1.36e-4 | 2.089 | 1.50e-5 | 2.997 |

**6.2. Stokes–Darcy coupling.** In this subsection, we consider a more general problem setting which is not covered by our theoretical results. The coupling of the Stokes problem with the Laplace equation plays in many applications an important role. Of special interest are porous media applications where the Darcy velocity can be used to describe a single-phase single-component transport. On the pore scale, the pore structure is resolved and the Navier-Stokes equations model the flow in the free-flow region and within the pores. On the "representative elementary volume" scale, however, the mathematical model can be considerably simplified by applying the potential theory resulting in Darcy's law in the porous media. Two-domain models exploit this observation and use suitable transfer conditions at the interface to couple the simple Darcy model for porous media with, e.g., the simplified Stokes equation in the free flow domain.

**6.2.1. Coupling Conditions.** In theory, the coupling conditions can be derived by applying volume-averaging techniques [10, 26]. In practice, however, simplified coupling conditions are often used. Here, we apply in tangential direction the Beavers–Joseph velocity-jump condition [2] in combination with the Saffman modification [20] (see also [11, 12]). This condition can be written as

$$\mathbf{u}_S \cdot \boldsymbol{\tau} - \frac{\sqrt{k}}{\gamma} 2\mathbf{n} \cdot \mathbf{D}(\mathbf{u}_S) \cdot \boldsymbol{\tau} = 0. \tag{6.1}$$

In normal direction, continuity of normal forces and mass conservation across the interface is assumed,

$$\mathbf{u}_S \cdot \mathbf{n} = \mathbf{u}_D \cdot \mathbf{n} \tag{6.2}$$

$$p_S - 2\mu \mathbf{n} \cdot \mathbf{D}(\mathbf{u}_S) \cdot \mathbf{n} = p_D, \tag{6.3}$$

see also [14]. The fluid velocities $\mathbf{u}_S$, $\mathbf{u}_D$ and pressure functions $p_S$, $p_D$ are defined on the Stokes and Darcy domains $\Omega_S$, $\Omega_D \subset \mathbb{R}^d$, respectively. The unit normal vector $\mathbf{n}$ points from $\Omega_S$ to $\Omega_D$, and $\boldsymbol{\tau}$ stands for the tangential vector on the interface. $\mathbf{D}(\mathbf{u}) := \left(\nabla \mathbf{u} + \nabla \mathbf{u}^T\right)/2$ stands for the deformation tensor. For a parameter $\mu > 0$ the value $k := \boldsymbol{\tau} \cdot \mu \mathbf{K} \cdot \boldsymbol{\tau}$ describes the dynamic viscosity, and $\mathbf{K}$ is a positive definite tensor that characterizes the intrinsic permeability of the porous medium. The parameter $\gamma > 0$ is a dimensionless constant that has to be determined experimentally.

**6.2.2. Numerical results.** For the numerical discretization we follow a hybrid discontinuous Galerkin approach based on mixed finite elements of possibly different orders in both subdomains [9, 13]. Here we consider the coupled Stokes-Darcy System on the unit-square $\Omega := (0, 1)^2$ which is subdivided into two subdomains

$$\Omega_S := (0, 1) \times (0.5, 1), \quad \Omega_D := (0, 1) \times (0, 0.5)$$

with the exact solution

$$\mathbf{u}_S = \left(\omega e^{\omega y}\sin(\omega x) + 2x^2\,(y-\xi) - 2G^3\,,\quad -\omega e^{\omega y}\cos(\omega x) - 2x\,(y-\xi)^2\right)^T,$$

$$\mathbf{u}_D = \left(\omega^2 e^{\frac{\omega}{2}}\sin(\omega x)y - G^2\,(y+0.5)^2\,,\quad -\omega e^{\frac{\omega}{2}}\cos(\omega x) - 2x\,(y+0.5)\,G^2\right)^T,$$

$$p_S = \omega e^{\frac{\omega}{2}}\cos(\omega x)\left(K^{-1}y - 2\omega\mu\right) + Gx\,(G-8\mu)\,,$$

$$p_D = K^{-1}\left(\omega e^{\frac{\omega}{2}}\cos(\omega x)y + x\,(y+0.5)^2\,G^2\right),$$

where $\mu := 1.0$ , $K := 1.0$ , $\gamma := 2.0$ , $G := \frac{\sqrt{K\mu}}{\gamma}$, $\omega := \frac{1}{2G}$ and $\xi := 0.5 - G$. The solution is chosen to fulfill the coupling conditions (6.1)–(6.3) on the interface $\Gamma = \overline{\Omega}_S \cap \overline{\Omega}_D$, and we assume that $\mathbf{K} = \mathrm{diag}(K)$. Note that the velocity has a continuous normal component on $\Gamma$ but is discontinuous in tangential direction. The domain is discretized by a sequence of uniformly refined quadrilateral meshes, where the numerical solution in $\Omega_S$ is computed by the Symmetric Interior Penalty Galerkin method using $BDM_h^{[k+1]}$ elements and in $\Omega_D$ we apply a mixed finite element method using $RT_h^{[k]}$ elements. We point out that the choice of the pairing is motivated by the idea of having the same order of convergence for the two subdomains. In Tables 6.7–6.8, the $L^2$-errors of the normal velocities on $\Gamma$ are listed for all refinement levels for $k = 0, 1$. In Figure 6.4, the normal velocities of the numerical solutions are plotted against the exact solution on two consecutive grid levels. Table 6.9 shows the $H^1(\Omega_S)$- and the $L^2(\Omega_D)$ errors for the velocities since these norms are natural given that the Stokes system is (essentially) a second order equation whereas the Darcy equation a first order system. The results show full convergence rates for both choices of $k$.

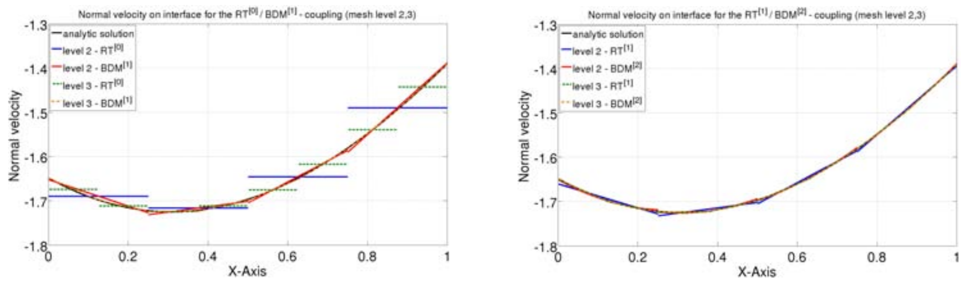


FIG. 6.4. *Numerical approximation of the normal velocity across the interface* $\Gamma$ *for the* $RT^{[0]}/BDM^{[1]}$ *- coupling (left) and the* $RT^{[1]}/BDM^{[2]}$ *- coupling (right)*

**Acknowledgement.** The research was carried out while JMM and BW attended the “special semester” on “Multiscale Simulation & Analysis in Energy and the Enviroment” hosted by the Johann Radon Institute for Computational and Applied Mathematics (RICAM) in Linz, October 3, 2011–December 15, 2011. The hospitality and financial support of the RICAM is very gratefully acknowledged.

**Appendix A. Regularity.** In Lemma 3.1, we showed assertion (iv) under the assumption of convexity of $\Omega$, i.e., under the assumption of full regularity. This assumption can be weakened: it suffices that $\Omega$ admits a shift theorem by more than 1/2 as we now show.

TABLE 6.7

*$L^2$-errors and convergence rates of the normal fluxes across the interface $\Gamma$ for the low-order solution (subscript L), solved with $RT_{[0]}/P_0$-element pair inside $\Omega_D$ and $BDM_{[1]}/P_0$-element pair inside $\Omega_S$.*

| level | $\mathbf{u}_S^L \cdot \mathbf{n}$ - error | rate | $\mathbf{u}_S^L \cdot \boldsymbol{\tau}$ - error | rate | $\mathbf{u}_D^L \cdot \mathbf{n}$ - error | rate |
|---|---|---|---|---|---|---|
| 1 | 1.48e-02 | - | 3.06e-02 | - | 2.77e-01 | - |
| 2 | 1.69e-03 | 3.125 | 3.48e-03 | 3.137 | 1.39e-01 | 1.000 |
| 3 | 2.68e-04 | 2.662 | 7.20e-04 | 2.273 | 6.94e-02 | 1.000 |
| 4 | 5.58e-05 | 2.262 | 1.63e-04 | 2.142 | 3.47e-02 | 1.000 |
| 5 | 1.33e-05 | 2.068 | 3.96e-05 | 2.045 | 1.73e-02 | 1.000 |
| 6 | 3.29e-06 | 2.016 | 9.81e-06 | 2.012 | 8.67e-03 | 1.000 |
| 7 | 8.20e-07 | 2.004 | 2.45e-06 | 2.002 | 4.33e-03 | 1.000 |

TABLE 6.8

*$L^2$-errors and convergence rates of the normal fluxes across the interface $\Gamma$ for the high-order solution (subscript H), solved with $RT_{[1]}/Q_1$-element pair inside $\Omega_D$ and $BDM_{[2]}/P_1$-element pair inside $\Omega_S$.*

| level | $\mathbf{u}_S^H \cdot \mathbf{n}$ - error | rate | $\mathbf{u}_S^H \cdot \boldsymbol{\tau}$ - error | rate | $\mathbf{u}_D^H \cdot \mathbf{n}$ - error | rate |
|---|---|---|---|---|---|---|
| 1 | 1.55e-02 | - | 2.29e-02 | - | 1.54e-02 | - |
| 2 | 1.68e-03 | 3.205 | 1.81e-03 | 3.656 | 1.71e-03 | 3.169 |
| 3 | 2.06e-04 | 3.028 | 1.96e-04 | 3.211 | 2.24e-04 | 2.930 |
| 4 | 2.53e-05 | 3.020 | 2.19e-05 | 3.162 | 3.38e-05 | 2.727 |
| 5 | 3.13e-06 | 3.014 | 2.54e-06 | 3.108 | 6.42e-06 | 2.396 |
| 6 | 3.89e-07 | 3.009 | 3.04e-07 | 3.064 | 1.45e-06 | 2.143 |
| 7 | 4.85e-08 | 3.005 | 3.70e-08 | 3.036 | 3.54e-07 | 2.040 |

TABLE 6.9

*mean $L^2$ and $H^1$-errors inside $\Omega_D$ and $\Omega_S$ respectively for the high- and low-order solution.*

| level | $\mathbf{u}_S^L$ - error | rate | $\mathbf{u}_D^L$ - error | rate | $\mathbf{u}_S^H$ - error | rate | $\mathbf{u}_D^H$ - error | rate |
|---|---|---|---|---|---|---|---|---|
| 1 | 1.05e-01 | - | 2.08e-01 | - | 1.06e-01 | - | 1.40e-02 | - |
| 2 | 2.57e-02 | 2.031 | 1.05e-01 | 0.991 | 2.36e-02 | 2.169 | 3.32e-03 | 2.077 |
| 3 | 7.68e-03 | 1.744 | 5.23e-02 | 0.998 | 5.74e-03 | 2.038 | 8.27e-04 | 2.007 |
| 4 | 2.80e-03 | 1.454 | 2.62e-02 | 0.999 | 1.42e-03 | 2.012 | 2.07e-04 | 2.001 |
| 5 | 1.23e-03 | 1.185 | 1.31e-02 | 1.000 | 3.55e-04 | 2.003 | 5.16e-05 | 2.000 |
| 6 | 5.92e-04 | 1.057 | 6.55e-03 | 1.000 | 8.87e-05 | 2.001 | 1.29e-05 | 2.000 |
| 7 | 2.93e-04 | 1.016 | 3.27e-03 | 1.000 | 2.22e-05 | 2.000 | 3.23e-06 | 2.000 |

For simplicity of exposition, we formulate this shift theorem as an assumption but point out that, for example, for $d = 2$ it is valid for polygonal Lipschitz domains $\Omega$.

ASSUMPTION A.1. . *Denote by $\widetilde{T}^D : H^{-1}(\Omega) \to H_0^1(\Omega)$ solution operator for the Poisson problem: Given $g \in H^{-1}(\Omega)$ find $y \in H_0^1(\Omega)$ such that*

$$-\Delta y = g \quad \text{in } \Omega, \qquad y = 0 \quad \text{on } \partial\Omega. \tag{A.1}$$

*There exists $s_0 > 1/2$ such that $\widetilde{T}^D$ is a bounded linear operator $\widetilde{T}^D : H^{-1+s_0}(\Omega) \to H^{1+s_0}(\Omega)$.*

We now show an analog of [16, Lemma 5.2]

LEMMA A.2. *Assume the validity of the shift theorem of Assumption A.1. Consider the variational problem: Given $g \in (L^2(\Omega))^d$, find $y \in H_0^1(\Omega)$ s.t.*

$$(\nabla y, \nabla z)_{0,\Omega} = (g, \nabla z)_{0,\Omega} \qquad \forall z \in H_0^1(\Omega). \tag{A.2}$$

*Then the solution operator $T^D : (L^2(\Omega))^d \to H_0^1(\Omega)$ given by $g \mapsto y$ extends to a bounded linear map*

$$T^D : \left((B_{2,1}^{1/2}(\Omega))^d\right)' \to B_{2,\infty}^{1/2}(\Omega).$$

*Proof. 1. step:* Our starting point is a very weak formulation. Fix $\varepsilon > 0$ such that $1/2+\varepsilon < s_0$. We introduce the bilinear form $B$ on $H^{1/2-\varepsilon}(\Omega) \times (H^{3/2+\varepsilon}(\Omega) \cap H^1_0(\Omega))$ by

$$B(y, v) := \langle y, -\Delta v\rangle_{1/2-\varepsilon,-1/2+\varepsilon}. \tag{A.3}$$

A few comments are in order: first, $\langle \cdot, \cdot\rangle_{1/2-\varepsilon,-1/2+\varepsilon}$ stands for the duality pairing between $H^{1/2-\varepsilon}(\Omega)$ and $H^{-1/2+\varepsilon}(\Omega)$. We point out that the assumption $\varepsilon > 0$ implies that $H^{1/2-\varepsilon}(\Omega) = H_0^{1/2-\varepsilon}(\Omega)$ so that the duality pairing is indeed well-defined. Second, from the mapping properties of $-\Delta$ (taken in the distributional sense) $-\Delta : H^2(\Omega) \to L^2(\Omega)$ and $-\Delta : H^1(\Omega) \to H^{-1}(\Omega)$, we get by interpolation that $-\Delta : H^{3/2+\varepsilon}(\Omega) \to H^{-1/2+\varepsilon}(\Omega)$ so that $B$ is indeed well-defined.
We claim that $B$ satisfies an inf-sup condition. To that end, let $u' \in C^\infty_0(\Omega)$ be arbitrary. By our assumptions on the mapping properties of $\widetilde{T}^D$ stated in Assumption A.1, there exists $v \in H^{3/2+\varepsilon}(\Omega) \cap H^1_0(\Omega)$ such that

$$(\nabla v, \nabla z)_{0,\Omega} = (u', z)_{0,\Omega} = \langle u', z\rangle_{-1/2+\varepsilon,1/2-\varepsilon} \qquad \forall z \in C^\infty_0(\Omega)$$

together with the bound $\|v\|_{3/2+\varepsilon,\Omega} \le C\|u'\|_{-1/2+\varepsilon,\Omega}$. By the definition of the distributional Laplacian, we obtain

$$B(z, v) = \langle u', z\rangle_{-1/2+\varepsilon,1/2-\varepsilon} \qquad \forall z \in C^\infty_0(\Omega).$$

Taking the supremum over $z \in C^\infty_0(\Omega)$, recalling the density of $C^\infty_0(\Omega)$ in $H^{1/2-\varepsilon}(\Omega) = H_0^{1/2-\varepsilon}(\Omega)$ and using the bound $\|v\|_{3/2+\varepsilon,\Omega} \le C\|u'\|_{-1/2+\varepsilon,\Omega}$, we get

$$\begin{aligned}\sup_{z\in C^\infty_0(\Omega)} \frac{B(z, v)}{\|z\|_{1/2-\varepsilon,\Omega}\|v\|_{3/2+\varepsilon,\Omega}} &= \sup_{z\in C^\infty_0(\Omega)} \frac{\langle u', z\rangle_{-1/2+\varepsilon,1/2-\varepsilon}}{\|z\|_{1/2-\varepsilon,\Omega}\|v\|_{3/2+\varepsilon,\Omega}} \\ &= \frac{\|u'\|_{-1/2+\varepsilon,\Omega}}{\|v\|_{3/2+\varepsilon,\Omega}} \ge C > 0.\end{aligned}$$

Furthermore, the bilinear form $B$ satisfies the "sup-sup" condition so that the bilinear form $B$ induces an isomorphism between $(H^{3/2+\varepsilon}(\Omega) \cap H^1_0(\Omega))'$ and $H^{1/2-\varepsilon}(\Omega)$.
*2. step:* Consider the problem: Given $g \in \left((H^{1/2+\varepsilon}(\Omega))^d\right)'$, find $y \in H^{1/2-\varepsilon}(\Omega)$ s.t.

$$B(y, z) = \langle g, \nabla z\rangle_{(H^{1/2+\varepsilon})'\times H^{1/2+\varepsilon}} \qquad \forall z \in H^{3/2+\varepsilon}(\Omega) \cap H^1_0(\Omega). \tag{A.4}$$

By the first step, the solution operator

$$T^D_{vw} : ((H^{1/2+\varepsilon}(\Omega))^d)' \to H^{1/2-\varepsilon}(\Omega) \tag{A.5}$$

given by $g \mapsto u$ is well-defined and a bounded linear operator. We next claim that $T^D_{vw}$ also has the mapping property

$$(L^2(\Omega))^d \to H^1_0(\Omega). \tag{A.6}$$

In fact, we will show the stronger statement

$$T^D_{vw} = T^D \qquad \text{on } (L^2(\Omega))^d.$$

To see this, let $g \in (L^2(\Omega))^d$. In order to see $y := T^D_{vw} g \in H^1(\Omega)$, let $\varphi \in (C^\infty_0(\Omega))^d$ and define $z_\varphi := \widetilde{T}^D(\nabla \cdot \varphi) \in H^{3/2+\varepsilon}(\Omega) \cap H^1_0(\Omega)$. We note the classical estimate

$\|z_\varphi\|_{1,\Omega} \leq C\|\varphi\|_{0,\Omega}$. We also observe that pointwise $-\Delta z_\varphi = \nabla \cdot \varphi$. Hence, an integration by parts together with the definition of the weak gradient $\nabla y$ yields:

$$\begin{aligned}\langle \nabla y, \varphi\rangle &\overset{def}{=} -(y, \nabla\cdot\varphi)_{0,\Omega} = (y, \Delta z_\varphi)_{0,\Omega} = -B(y, z_\varphi) \overset{(A.4)}{=} \langle g, \nabla z_\varphi\rangle_{(H^{1/2+\varepsilon})'\times H^{1/2+\varepsilon}} \\ &= (g, \nabla z_\varphi)_{0,\Omega}.\end{aligned}$$

For the right-hand side, we have $|(g, \nabla z_\varphi)_{0,\Omega}| \leq \|g\|_{0,\Omega}\|\nabla z_\varphi\|_{0,\Omega} \leq \|g\|_{0,\Omega}\|\varphi\|_{0,\Omega}$. Hence, $\nabla y \in L^2(\Omega)$.
As a next step towards showing that $y = T^D_{wv} g = T^D g =: \widetilde{y}$, we show that $y - \widetilde{y}$ is harmonic. To that end, let $\varphi \in C^\infty_0(\Omega)$. Then

$$\begin{aligned}\langle -\Delta(y-\widetilde{y}), \varphi\rangle &\overset{def}{=} (y-\widetilde{y}, -\Delta\varphi)_{0,\Omega} = B(y,\varphi) - (\nabla\widetilde{y}, \nabla\varphi)_{0,\Omega} \\ &= (g, \nabla\varphi)_{0,\Omega} - (g, \nabla\varphi)_{0,\Omega} = 0.\end{aligned}$$

Next, we show $y \in H^1_0(\Omega)$. In order to establish this, we note that, since $-\Delta(y-\widetilde{y}) = 0$, the co-normal derivative $\partial_n(y-\widetilde{y})$ is a well-defined element of $H^{-1/2}(\partial\Omega)$ given by the following relation for all $\varphi \in C^\infty_0(\overline{\Omega})$:

$$\begin{aligned}0 &= \langle \partial_n(y-\widetilde{y}), \varphi\rangle = (\nabla(y-\widetilde{y}), \nabla\varphi)_{0,\Omega} = (y, \partial_n\varphi)_{0,\partial\Omega} - (y, \Delta\varphi)_{0,\Omega} - (\nabla\widetilde{y}, \nabla\varphi)_{0,\Omega} \\ &= (y, \partial_n\varphi)_{0,\partial\Omega} + B(y,\varphi) - (g, \nabla\varphi)_{0,\Omega} = (y, \partial_n\varphi)_{0,\partial\Omega}.\end{aligned}$$

By varying $\varphi \in C^\infty_0(\Omega)$, we conclude that $y = 0$ on $\partial\Omega$.
We have thus shown that the very weak solution $y = T^D_{vw} g \in H^1_0(\Omega)$ if $g \in L^2(\Omega)$. An integration by parts then shows that $y$ solves the weak formulation, and uniqueness of the weak solution thus provides $y = \widetilde{y}$. This shows that $T^D_{vw}$ is the unique extension of $T^D$ to $((H^{+1/2+\varepsilon}(\Omega))^d)'$.
*3. step:* The above steps have shown that $T^D_{vw}$ has the following mapping properties:

$$T^D_{vw} : ((H^{1/2+\varepsilon}(\Omega))^d)' \to H^{1/2-\varepsilon}, \qquad T^D_{vw} : (L^2(\Omega))^d \to H^1_0(\Omega)$$

By a standard interpolation argument, $T^D_{vw}$ is a bounded linear operator

$$T^D_{vw} : ((L^2)^d, ((H^{1/2+\varepsilon})^d)')_{\theta,\infty} \to (H^1_0, H^{1/2-\varepsilon})_{\theta,\infty} \subset (H^1, H^{1/2-\varepsilon})_{\theta,\infty}$$

for every $\theta \in (0,1)$. Select $\theta \in (0,1)$ such that $1/2 = \theta(1/2+\varepsilon)$. Then $(H^1, H^{1/2-\varepsilon})_{\theta,\infty} = B^{1/2}_{2,\infty}(\Omega)$. Furthermore, by [22, Thm. 1.11.2] or [21, Lemma 41.3]

$$\left((B^{1/2}_{2,1}(\Omega))^d\right)' = \left(((L^2)^d, (H^{1/2+\varepsilon})^d)_{\theta,1}\right)' = \left((L^2)^d, ((H^{1/2+\varepsilon})^d)'\right)_{\theta,\infty}$$

We conclude that $T^D_{vw}$ is a bounded linear operator from $\left((B^{1/2}_{2,1}(\Omega))^d\right)'$ to $B^{1/2}_{2,\infty}(\Omega)$. As we have already ascertained that $T^D_{vw} = T^D$ on $(L^2(\Omega))^d$, the proof is complete. ◻
Lemma A.3. *Let $\Omega$ satisfy Assumption A.1 Then the operator $T^M_w$ of Lemma 3.1 is a bounded linear operator*

$$T^M_w : \left((B^{1/2}_{2,1}(\Omega))^d\right)' \to B^{1/2}_{2,\infty}(\Omega).$$

*Proof.* The proof follows by observing that on $(L^2(\Omega))^d$, the operator $T^M_w$ coincides with the weak solution operator $T^D$ of Lemma A.2, which has the stated mapping property. ◻

## REFERENCES


[1] D. Arnold and F. Brezzi. Mixed and nonconforming finite element methods: Implementation, postprocessing and error estimates. *RAIRO, Modélisation Math. Anal. Numér.*, 19:7–32, 1985.

[2] G. Beavers and D. Joseph. Boundary conditions at a naturally permeable wall. *J. Fluid Mech.*, 30:197–207, 1967.

[3] F. Brezzi. A survey of mixed finite element methods. In *Finite elements. Theory and application, Proc. ICASE Workshop*, pages 34–49. Hampton/VA 1986, 1989.

[4] F. Brezzi. Stability of saddle-points in finite dimensions. In *Frontiers in numerical analysis. 10th LMS-EPSRC numerical analysis summer school, Durham, UK, July 7-19, 2002*, pages 17–61. Berlin: Springer, 2003.

[5] F. Brezzi, J. Douglas, and L. Marini. Two families of mixed finite elements for second order elliptic problems. *Numer. Math.*, 47:217–235, 1985.

[6] F. Brezzi, J. Douglas, and L. Marini. Recent results on mixed finite element methods for second order elliptic problems. In *Vistas in applied mathematics. Numerical analysis, atmospheric sciences, immunology*, pages 25–43. dedic. G. I. Marchuk occas. 60th birthday, 1986.

[7] F. Brezzi and M. Fortin. *Mixed and hybrid finite element methods*. Springer, New York, 1991.

[8] L. Gastaldi and R. Nochetto. Sharp maximum norm error estimates for general mixed finite element approximations to second order elliptic equations. *RAIRO Modél. Math. Anal. Numér.*, 23(1):103–128, 1989.

[9] V. Girault and B. Riviere. Dg approximation of coupled Navier–Stokes and Darcy equations by Beaver–Joseph–Saffman interface condition. *J. Numer. Anal.*, 47:2052–2089, 2009.

[10] W. Gray, A. Leijnse, R. Kolar, and C. Blain. *Mathematical tools for changing spatial scales in the analysis of physical systems.* CRC Press, 1993.

[11] W. Jäger and A. Mikelic. On the interface boundary condition of Beavers, Joseph and Saffman,. *SIAM J. Appl. Math.*, 60:1111–1127, 2000.

[12] W. Jäger and A. Mikelic. Modeling effective interface laws for transport phenomena between an unconfined fluid and a porous medium using homogenization. *Transp. Porous Media*, 78:489–508, 2009.

[13] G. Kanschat and B. Riviere. A strongly conservative finite element method for the coupling of Stokes and Darcy flow. *J. of Comput. Phys.*, 229:5933–5943, 2010.

[14] W. Layton, F. Schieweck, and I. Yotov. Coupling fluid flow with porous media flow. *SIAM J. Numer. Anal.*, 40:2195–2218, 2002.

[15] J. Li, J.M. Melenk, B. Wohlmuth, and J. Zou. Optimal a priori estimates for higher order finite elements for elliptic interface problems. *Appl. Numer. Math.*, 60:19–37, 2010.

[16] J.M. Melenk and B. Wohlmuth. Quasi-optimal approximation of surface based Lagrange multipliers in finite element methods. Technical Report 13, Inst. for Analysis and Sci. Computing, Vienna Univ. of Technology, 2011.

[17] J. Nedelec. Mixed finite elements in $\mathbb{R}^3$. *Numer. Math.*, 35:315–341, 1980.

[18] R. Nicolaides. Existence, uniqueness and approximation for generalized saddle point problems. *SIAM J. Numer. Anal.*, 19:349–357, 1982.

[19] P. Raviart and J. Thomas. A mixed finite element method for 2nd order elliptic problems. In *Math. Aspects Finite Elem. Meth., Proc. Conf. Rome 1975,*, pages 292–315. Lect. Notes Math. 606, 1977.

[20] R. Saffman. On the boundary condition at the surface of a porous medium,. *Stud. Appl. Math.*, 50:93–101, 1971.

[21] L. Tartar. *An introduction to Sobolev spaces and interpolation spaces*, volume 3 of *Lecture Notes of the Unione Matematica Italiana*. Springer, Berlin, 2007.

[22] H. Triebel. *Interpolation theory, function spaces, differential operators.* Johann Ambrosius Barth, Heidelberg, second edition, 1995.

[23] L. Wahlbin. Local behavior in finite element methods. In P.G. Ciarlet and J.L. Lions, editors, *Handbook of numerical Analysis. Volume II: Finite element methods (Part 1)*, pages 353–522. North Holland, 1991.

[24] L. Wahlbin. *Superconvergence in Galerkin finite element methods*, volume 1605 of *Lecture Notes in Mathematics*. Springer Verlag, 1995.

[25] J. Wang. Asymptotic expansions and $L^\infty$-error estimates for mixed finite element methods for second order elliptic problems. *Numer. Math.*, 55(4):401–430, 1989.

[26] S. Whitaker. *The method of volume averaging*, volume 240. Kluwer Academic Publishers, 1999.

[27] P. Wriggers and C. Carstensen, editors. *Mixed finite element technologies.*, volume CISM Courses and Lectures 509. Wien: Springer, 2009.